2012

Characterization of Elastic-Like Polypeptide Micelles Using Capillary Viscometry

Sumit H. Kambow
Cleveland State University

CHARACTERIZATION OF ELASTIN-LIKE POLYPEPTIDE MICELLES USING CAPILLARY VISCOMETRY

SUMIT H. KAMBOW

Bachelor of Technology in Chemical Engineering

Punjab Technical University

May 2008

submitted in partial fulfillment of requirements for the degree

MASTER OF SCIENCE IN CHEMICAL ENGINEERING

at the

CLEVELAND STATE UNIVERSITY

May 2012

This thesis has been approved for the Department of Chemical and Biomedical Engineering and the College of Graduate Studies by

_____

Dr. Nolan B. Holland
Department of Chemical and Biomedical Engineering
Cleveland State University

_____
Date

_____

Dr. Rolf Lustig
Department of Chemical and Biomedical Engineering
Cleveland State University

_____
Date

_____

Dr. Dhananjai B. Shah
Department of Chemical and Biomedical Engineering
Cleveland State University

_____
Date

ACKNOWLEDGMENTS

I would like to express my sincere gratitude to my academic advisor Dr. Nolan B. Holland for the research opportunity that he provided me at his laboratory. He taught me valuable lessons and his continuous support, patience, encouragement, and guidance are invaluably appreciated.

I would also like to extend my regards to my committee members Dr. Dhananjai B. Shah and Dr. Rolf Lustig for their valuable support and advice. Thanks also go out to the faculty and the staff of the Chemical and Biomedical Engineering Department at Cleveland State University for the family atmosphere that I and many other international students are experiencing on a daily basis. Special thanks are paid to Ms. Becky Laird and Darlene Montgomery for their continuous support throughout my stay at Cleveland State University. My colleagues at the laboratory were always supportive and I would like to gratefully thank them.

Lastly and most importantly, I would sincerely like to thank my parents, Harbhajan Singh and Amarjeet Kaur for their constant support throughout the completion of my academic career. They raised me, taught me, and loved me. To them I dedicate this thesis.

CHARACTERIZATION OF ELASTIN-LIKE POLYPEPTIDE MICELLES USING CAPILLARY VISCOMETRY

SUMIT H. KAMBOW

ABSTRACT

Elastin-like polypeptides (ELPs) are a part of the family of responsive polymers. These polymers can be made to respond to a wide variety of stimuli, including temperature, pH, salt concentration, light, and solvent. Elastin-like polypeptides are soluble in water at low temperatures but they become hydrophobic and insoluble above their transition temperature. Elastin-like polypeptides, $(GVGVP)_{40}$-foldon and $(GVGVP)_{60}$-foldon, were expressed in bacterial system. These ELPs above their transition temperature, T_t, at low salt (< 45 mM), and high pH (> pH 10) assemble into micelles where the hydrophobic tails phase separate in the interior of the micelle as an immiscible coacervate phase. The oligomerization domain termed as foldon, has a net negative charge and behaves as a hydrophilic group to stabilize the aggregates formed by the ELP chains above their transition temperature. The coacervate, which makes up interior of micelles, contains 37% protein and 63% water when it is in a bulk state. The aim of my research was to find out the density of protein in the micelle by using capillary viscometry. We used Ubbelohde capillary viscometer to calculate the relative viscosity of ELPs which was used to calculate the intrinsic viscosities using Kraemer and Huggins equations. The micelles at low salt concentration and high pH are spherical therefore we use equivalent sphere model to calculate the density of protein per micelle from intrinsic viscosity. Using this model we calculated the density of protein per micelle to be 0.26 g/ml. Using our micelle model and data from light scattering, we calculated the density of

protein in the coacervate to be 40% and rest water. There were two limitations in this project. First, specific viscosities at low concentrations were small with large errors. The second limitation was controlling the pH of the polymer solutions during the experiments. The pH of polymer solution could not easily be monitored once the sample was loaded in the viscometer.

TABLE OF CONTENTS

LIST OF TABLES

LIST OF FIGURES

CHAPTER I

INTRODUCTION AND BACKGROUND

1.1 Introduction

Elastin- like polypeptides (ELPs) are environmentally responsive biopolymers that have recently emerged as a promising new class of materials. The properties of these molecules are derived from their amino acid sequence which imparts biological activity and often determines the biodegradation of the polypeptide. They are attractive because their genetically encoded synthesis provides control over sequence, chain length, and stereochemistry, which is unattainable to this level using chemical polymerization techniques. The sequence and molecular weight are of particular importance because these determine the physicochemical properties and *in vivo* applications. With advances in molecular biology techniques and recombinant DNA technology it has become possible to create a wide range of materials based on specific amino acid sequences [1]. The synthesis of these synthetic genes leads to the production of genetically engineered protein based polymers (PBPs). The diversity and structural control makes these protein-

based polymers unmatchable among the known polymers. Elastin-like polypeptides are based on repeats of the pentapeptide (GαGβP) in which α can be any of the 20 naturally occurring amino acids while β can be any of those amino acids except proline. The polymer $(GVGVP)_n$ is considered as a model for studying and developing the principles of free energy transduction for protein based polymers [2].

1.2 Elastin-like Polypeptides

Elastin is a polymeric protein that imparts extensibility and elastic recoil to large blood vessels, lung parenchyma, and skin [3]. Elastin-like polypeptides (ELPs) can go into an organized self-assembled structure. They are responsive materials and exhibit conformational changes due to their sensitivity to slight changes in the surrounding environment such as changes in temperature, pH, etc. ELPs show a reversible phase transitional behavior in response to temperature. This behavior is known as an inverse transition temperature (T_t) [3]. A polypeptide consists of amino acids covalently bonded to each other (Figure 1.1) [4]. This chemical covalent bond is the peptide bond formed between two molecules when the carboxyl group of one molecule reacts with amine group of other molecule, causing the release of a molecule of water. A chain of peptide always has an amino group at one end (N-terminus) and a carboxyl group at the other end (C-terminus). An amino acid can be represented by their single-letter codes, with the protein sequence written from N-terminus to C-terminus.

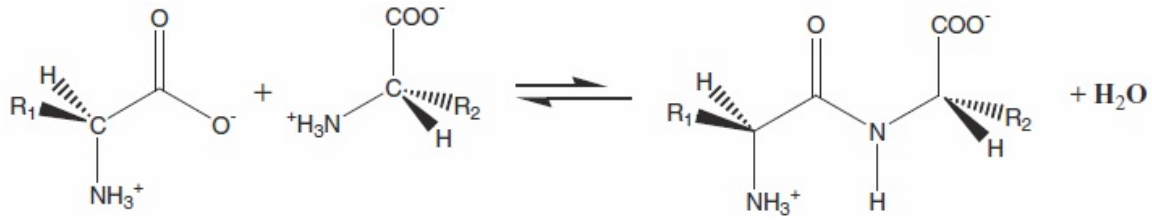

Figure 1.1.: Peptide bond formation from two amino acids (reproduced from reference [4] with permission).

One of the most important properties of ELPs is that they are soluble in solution below their transition temperature, and phase separate above their transition temperature. This behavior of ELPs is useful in many ways such as purifying them by separating the aggregate from the contaminants using centrifugation above the T_t [5].

1.3 Applications of ELPs

ELPs are suitable for application as protein purification tags, targeted drug delivery carriers, self-assembled and chemically cross-linked tissue engineering scaffolds, and as components of biosensing and bioanalytical devices [6-7]. There has been increased attention for utilizing these polymers for biomedical applications because they can be non-toxic, biocompatible, biodegradable, and they have also displayed good pharmacokinetics [6,8,9]. Because of the phase transitional behavior shown by ELPs, proteins with ELP tags can be purified by inverse thermal cycling, which avoids many problems associated with chromatography-based methods.

Thermosensitive properties of ELPs make them an interesting class of polypeptides for use in drug delivery. ELPs can be used as polymeric carriers for anticancer therapeutics because they are likely to maintain biocompatibility throughout

the degradation process. Amphiphilic polypeptides such as micelles can be used to trap drugs and they can be targeted to tissues by applying external hyperthermia. Adam and co-workers demonstrated the local delivery of antibiotics using ELPs [10]. Other research has focused on targeting cancer medicine to tumors utilizing ELPs as drug carriers. Since the tumor has a reduced pH, as low as 6.3 for cells with carcinoma and 6.8 for cells with melanoma, in comparison to the pH level in healthy tissues which is 7.35, the sensitivity of the ELPs to pH level can play a significant role in the treatment of such cells [11,12].

Chilkoti *et al.* synthesized two ELPs of different compositions with one having a higher T_t than the other due to higher hydrophilic character. ELP1 had a T_t that was approximately 37 °C and ELP2 had a T_t that was approximately 42 °C. The ELPs were injected into nude mice which contained human tumor xenografts and these were monitored by intravital microscopy. This imaging technique showed that ELP1 aggregated within the blood of tumors that were heated. ELP2 did not aggregate under these conditions. This was the first study to demonstrate that an ELP would undergo phase transition inside a tumor at a desired temperature [6,13-14]. Peptide based biomaterials are useful for tissue engineering because they have good chemical compatibility and they break down into natural amino acids that can be metabolized by the body. They are mainly used as injectable scaffolds that form hydrogels inside the human body and can serve as artificial extracellular matrix to provide embedded cells for tissue repair.

1.4 Temperature Dependence of ELPs

ELPs undergo a reversible phase transition referred to as the inverse temperature transition or lower critical solution temperature (LCST) behavior (Figure 1.2). At 20 °C, the polypeptide and water are miscible in all proportions. On raising the temperature to 30 °C when there is more than 63% water by weight, there is a phase separation (coacervation occurs) with the development of an equilibrium solution. The composition of the coacervate at 30 ^{o}C is 37% peptide and 63% water by weight. Continuing to raise the temperature to 60 ^{o}C shows only a small amount of change in the phases such that at 60 °C the composition is 38% peptide and 62% water by weight. Very interestingly above 60 °C there is a dramatic expulsion of water from the coacervate and at 80 °C it has a composition of 68% peptide and 32% water by weight. The entire process is reversible [15].

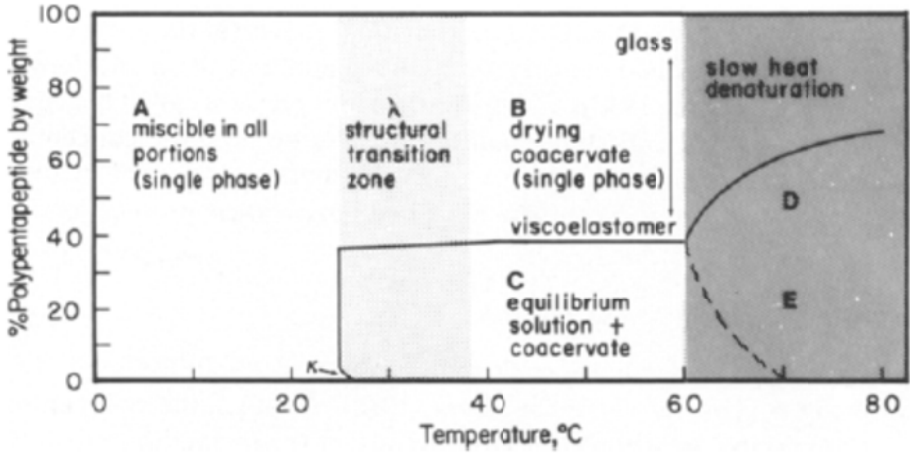

Figure 1.2: Phase diagram of the polypentapeptide-water system (reproduced with permission from reference [18]).

1.5 Factors Affecting Transition Temperature (T_t)

One of the features of ELPs is the ability to alter the transition temperature based on chain length, polymer concentration, polymer composition, solution composition, pH, side chain charge and light. In this study we investigated the effects of chain length, polymer concentration, and solution composition; however some of the other effects will be briefly discussed here. The functionality of $(GVGVP)_n$ will be maintained as long as the glycine and proline residues are left in place, which leads to the ability to substitute for the valines: poly $(G\alpha G\beta P)_n$. The α position can be filled with any of the 20 natural amino acids. The β position can also be replaced with any of the natural amino acids, except for proline due to the nature of the formation of β-turns between glycine and proline residues. Changing the polarity or the hydrophobicity of the ELP will change the T_t. Urry was able to develop a T_t -based hydrophobicity scale which illustrated the effects of substituting amino acids under common solvent conditions [2]. The results indicate that the more hydrophobic the substitution was the more it depressed the T_t ; higher values of T_t were indicative of side chains more polar than valine.

ELPs can also be pH responsive and this is due to the fact that the T_t of all ELPs depends on the mean polarity of the polymer [16]. The γ-carboxylic group of E showed large polarity changes when the pH changes. At pH 2.5 the T_t was found to be 28 °C and at pH 8.0 the T_t was 85 °C. The design of this ELP contained just 4 glutamic acid residues per 100 amino acids in the polymer backbone, which was enough to affect a difference of 57 °C in the T_t between pH states.

1.6 Methods to Vary the Transition Temperature of ELPs

ELPs below T_t, remain soluble in the aqueous solution. On the contrary, they hydrophobically fold and assemble to form a phase-seperated state above T_t. This section details the methods that are used to alter the T_t of ELPs. These methods include, ELP concentration, ELP chain length and solution parameters such as NaCl concentration.

1.6.1 Effect of NaCl on T_t of ELPs

Reguera *et al.* showed the effect of NaCl on the exothermic and endothermic components of the LCST [17] by making use of temperature modulated differential scanning calorimetry (TMDSC), a technique that is able to separate the two components [18]. NaCl causes a significant and concentration dependent decrease in the LCST [17] as well as an increase in the transition enthalpy (ΔH_t) (Figure 1.3). Typical DSC thermograms show a decrease in the T_t with increasing NaCl concentration and the area under the endotherm is taken as the enthalpy. The endothermic peak of a DSC was described as an increase in the order of the system by increasing the waters of hydrophobic hydration. Exothermic behavior is described as the folding and association while the endothermic behavior is the disruption of ordered water structures. Both of these components increase with the addition of NaCl. The total effect is explained as an increase in the hydrophobicity of the chain, which causes a decrease in T_t and an increase in the enthalpy. The authors conclude that the effect of NaCl is to cause increased organization of ELPs in the folded state and an improved structure of hydrophobic hydration surrounding the chain [18].

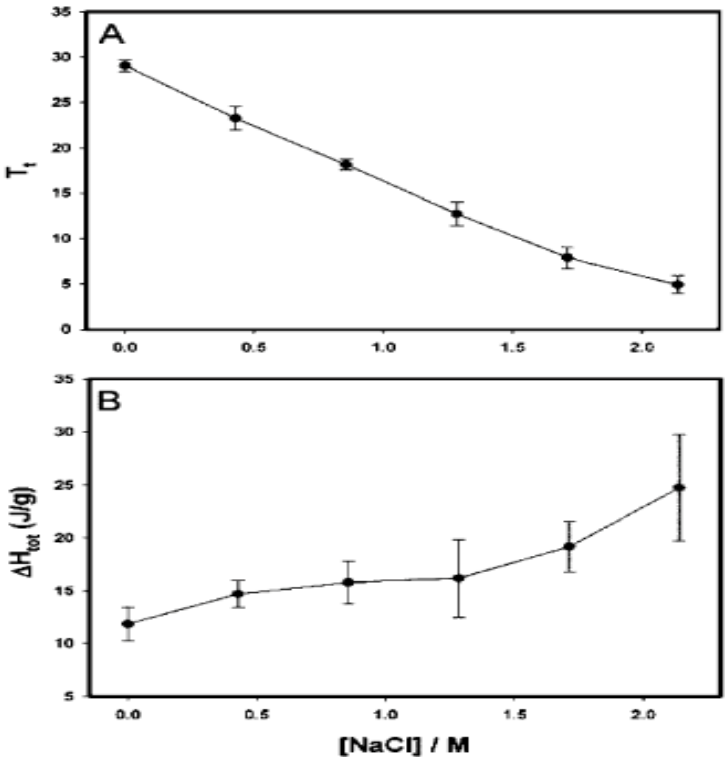

Figure 1.3.: Influence of the salt concentration on the T_t (A) and enthalpy (B) for a 50 mg/mL $(GVGVP)_{251}$ aqueous solution (reproduced with permission from reference [17]).

Nuhn and Klok [19] showed the secondary structure formation and T_t behavior of short ELPs. This study focused on the T_t behavior of ELPs ranging in length from 1 to 6 pentapeptide repeats. Other studies have focused on this behavior [20,21,22] but have not focused on multiple factors effecting T_t. For very short ELPs the T_t may not be measurable in UV-vis spectrophotometers due to the temperature control limits. Typical UV-vis spectrophotometers are able to operate in the range of 10 to-100 °C. To overcome these equipment limitations the authors added NaCl in various concentrations to the ELP and extrapolated to zero NaCl concentration to find the reported T_t value [19]. Protein solutions were measured at 10 mg/ ml and the T_t of $(GVGVP)_5$ was found to be 124 °C at 0 M NaCl and report an T_t of 40 °C at 3 M NaCl concentration. This large difference is much higher than that reported for ELPs of higher molecular weight [23]. In a study

based on higher molecular weight ELPs, Urry *et al.* reported a linearly dependent decrease of T_t on NaCl concentration, but the reported difference was 14 °C / per repeat unit [23]. The authors concluded from this that the T_t values of short ELPs are more sensitive to the addition of NaCl than longer chains.

Yamoka *et al.* investigated the effects of the addition of NaCl and other additives such as SDS on the T_t of $(VPGIG)_{40}$ [24]. With the addition of increasing NaCl, KCl and K_2SO_4 concentrations there was a linear decrease in T_t. The addition of SDS at different concentrations was shown to have a strong effect on the LCST behavior. Adding SDS at values higher than the critical micelle constant of SDS [25] caused the disappearance of T_t, while values of SDS lower than CMC caused a gradual increase in T_t. The authors explained these effects in the following way. Salts, such as NaCl that have a lower lyotropic numbers induce the globular state of polymers [26]. These salts act in a manner that strengthens the hydyophobic interactions which allow ELPs to hydrophobically fold and assemble and thus lower the LCST [24].

Researchers have shown a linear relationship between T_t and salt concentrations [19,27]. Ghoorchian *et al.* also showed the linearity of T_t as a function of NaCl concentration for $(GVGVP)_{40}$, $(GVGVP)_{40}$-foldon, and $(GVGVP)_{120}$ (Figure 1.4) [27], except at low salt concentrations i.e. below 45 mM. The slope for the $(GVGVP)_{40}$-foldon and $(GVGVP)_{120}$ are the same with higher temperature values for the construct with the foldon. If the amount of salt is increased, the ionic strength of the solution increases leading to an increase in the polarity difference between water molecules and the hydrophobic components and therefore the ELP precipitates at lower temperatures [28].

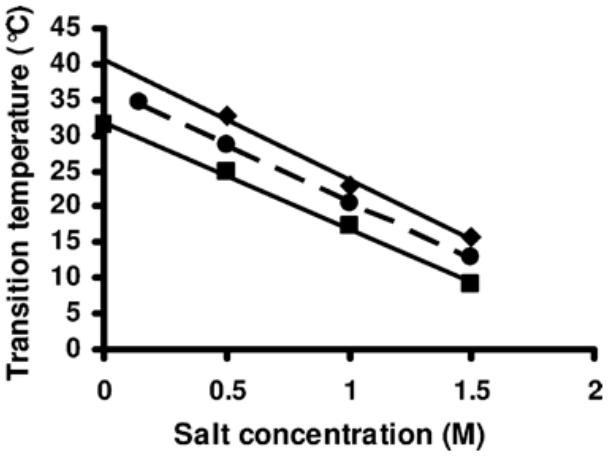

Figure 1.4.: Effect of salt on the transition temperature of $(GVGVP)_{40}$ (diamonds), $(GVGVP)_{40}$-foldon (circles), and $(GVGVP)_{120}$ (squares) (reproduced with permission from reference [27]).

1.6.2 Effect of ELP Concentration and Chain Length on T_t

Effects of peptide concentration on the LCST behavior of ELPs have been extensively studied and shown to have strong effects. Urry described the phase behavior related to ELPs [28] and showed that there is strong concentration dependence. He found that, at low ELP concentrations there is a dramatic increase in T_t and his concept was also supported by the work of Meyer and Chilkoti [29]. They also described T_t dependence on chain length, concentration and specific constants and showed that the concentration and chain length have a great impact on T_t of ELPs that are of low peptide concentration and of small chain length. It has been shown that ELPs of shorter chain length have higher T_t values than larger chain lengths [19,29]. Urry described the effects of ELP concentration on T_t in two ways [30]. First, at low ELP concentrations the T_t increased because the interchain cooperativity needed for ELPs to fold correctly does not take place efficiently in dilute peptide conditions. Second, at extremely high concentrations there was an inability for the ELP to go from the unfolded state to the completely hydrated folded state

[30]. This situation also causes an increase in T_t. Cabello and Reguera showed that the T_t decreased as the molecular weight increased [16]. They also showed that the transition enthalpy increased with increase in molecular weight of ELPs.. The overall effect of increasing the molecular weight was seen to be similar to the changes seen in changing the mean polarity of the ELPs such that lowering the molecular weight is similar to decreasing the mean hydrophobicity of the ELP.

1.6.3 Effect of pH on T_t

MacKay *et al.* developed a quantitative model to describe the phase behavior of pH-responsive ELPs that uses the Henderson-Hasselbalch relationship [31]. They designed pH-responsive ELPs that contained either acidic or basic residues. The acidic ELPs are charged above their pK_a and they have high T_t. When their pH is below their pK_a, the acidic residues become protonated and neutral leading to a decrease in their T_t . On the other hand, the basic ELPs at low pH are soluble and when their pH increases above their pK_a, they neutralize leading to a decrease in their T_t. Their results were useful in describing the phase transition behavior of ELPs in response to a specified change in pH as the trigger.

1.7 ELP Micelles

Polymeric micelles can be used as carriers for hydrophobic drugs or genes. They consist of two blocks with differing polarity and form nanoparticles in response to changes in their environment. The hydrophobic core can be used to trap hydrophobic compounds and increase their solubility in an aqueous environment. ELPs are soluble in

water at low temperatures, but above transition temperature they become insoluble. Above transition polypeptides form large particles that separate into a second phase [27]. Ghoorchian *et al.* modified this response by adding a charged trimer- forming domain. This domain connects three ELP chains together and adds a hydrophilic head group. This effectively makes a surfactant when the ELP chains are in a hydrophobic state. When above the transition temperature this system acts like a surfactant and forms micelles (Figure 1.5). Micelles are small aggregates where the hydrophobic head groups surround the hydrophobic core.

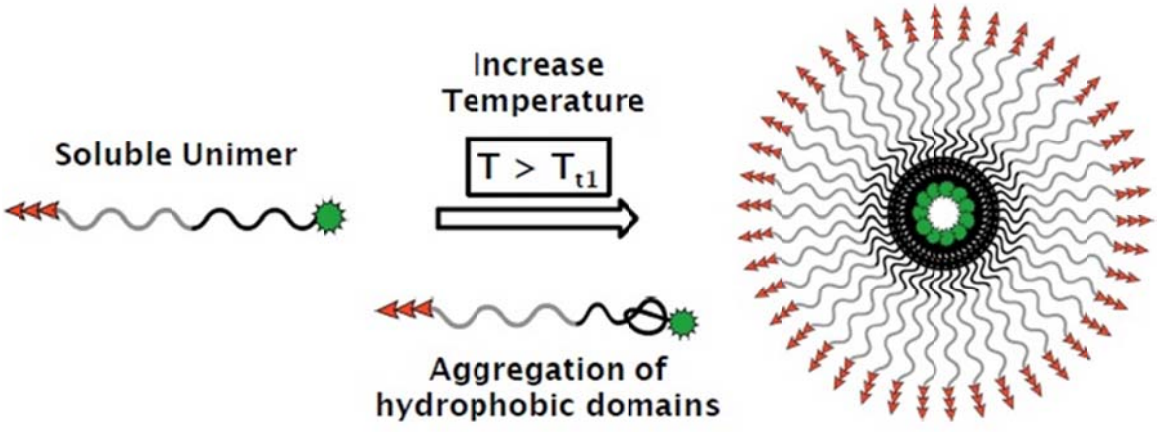

Figure 1.5: Above T_t polypeptide chains become hydrophobic and aggregate into micelles stabilized by charged oligomerization domain (reprinted with permission from reference [32]).

The foldon domain has a net negative charge and so can behave as a hydrophilic group to stabilize the coacervate aggregates formed by the ELP chains above their transition temperature. In essence, the ELP-foldon is a surfactant with three hydrophobic tails and a charged headgroup,which forms micelles at salt concentrations below 45 mM (Figure 1.6). The salt concentration plays a key role in determining the size and type of aggregation that occurs in charged surfactant systems. The primary effect of salt in

solution is to moderate the electrostatic interactions between charged species, however, salt can also modify hydrophobic interactions as is observed by the dependence of the transition temperature of ELPs on salt. As the salt concentration increases above 50 mM and we move into regime III (Figure 1.6) , the charge on the foldon domains is shielded to a greater extent so that large aggregates will form.

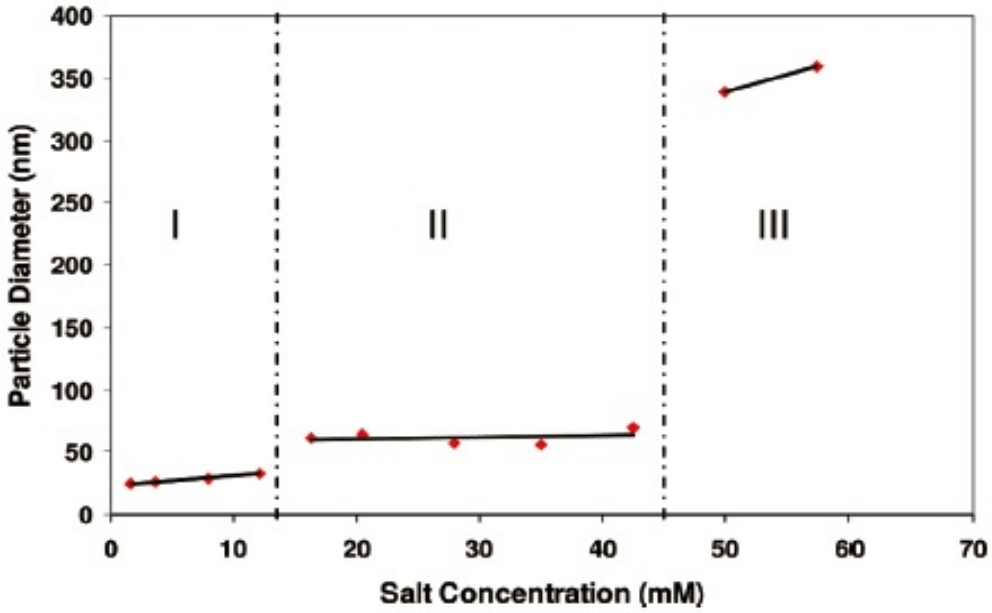

Figure 1.6.: Dynamic light scattering of $(GVGVP)_{40}$-foldon in different NaCl concentrations. Dynamic light scattering was performed on 10 μM polypeptide solutions at 50 ^{o}C, which is above the polypeptide transition temperature. The measurements show very narrow distribution of particle sizes over a wide range of salt concentrations and that the size of the aggregates varies as a function of salt concentration. (reprinted with permission from reference [27])

Chilkoti *et al.* synthesized a series of 10 ELP block copolymers with a range of molecular weights and hydrophilic-to-hydrophobic ratios. ELPs with hydrophilic-to-hydrophobic ration between 1:2 and 2:1 formed monodisperse spherical micelles. The size of these micelles was controlled by both the total ELP length and hydrophilic- to-hydrophobic block ratio. These polypeptide micelles displayed a critical micelle

concentration in the range of 4 to 8 μM, indicating that these structures are highly stable [33]. Furthermore, the microviscosity of these ELPs increased as they self-assembled into a micelle from unimers. The microviscosity of the micelles was greater than the bulk aggregate, suggesting that the micellar structure was altered during reorganization into the micron size aggregates of the coacervate that occured at the second thermal transition. Their study was the first demostration of temperature triggered multivalency that ELPs presenting biologically relevant peptide ligands self- assembled into spherical micelles at a clinically- relevant temperature.

1.8 Characterization of ELPs

Many techniques have been used over the years to characterize the solution properties of peptides and proteins. The following section will briefly discuss the methods to characterize ELPs. Later, we will discuss about the characterization of ELPs using capillary viscometry which has been used for this study.

1.8.1 Biophysical Properties

Protein concentration of peptide-based biomaterials can be determined by UV spectroscopy. ELPs show inverse temperature transition behavior which is often determined by the turbidity (optical density at 350 nm) as a function of temperature [34,35,36]. Molecular weight of these materials can be measured by SDS-PAGE, mass spectrometry (MS) methods such as matrix-assisted laser desorption ionization (MALDI-MS) and electrospray MS [8]. Isothermal titration calorimetry (ITC) is used to study the thermodynamic parameters such as binding enthalpy, entropy, free energy, and binding

constant. Binding behavior of peptide based biomaterials can be determined using surface plasmon resonance spectroscopy (SPR).

1.8.2 Structural Properties

Structural properties of ELPs play an important role in protein purification, tissue engineering, and drug delivery applications. Structural properties such as hydrodynamic radius of polypeptides in aqueous solution can be determined by dynamic light scattering (DLS). DLS is also very useful in examining the formation of polypeptide micelles. Protein folding can be studied using circular dichroism spectrometry (CD) and differential scanning microcalorimetry (DSC) [36,37].

1.8.3 Characterization of ELP micelles using capillary viscometry

Viscometry is one of the simplest and cheapest methods to examine the structure and the properties of a polymeric solution. In these experiments, a dilute solution flows through a capillary tube (Figure 1.7) [39]. The flow velocity, and shear rate, are different depending on the distance from the edge of the capillary. The polymer molecule undergoes a different shear rate within its coil which results in an increase in the frictional drag and rotational forces on the molecule, which increases the viscosity of polymer in the solution.

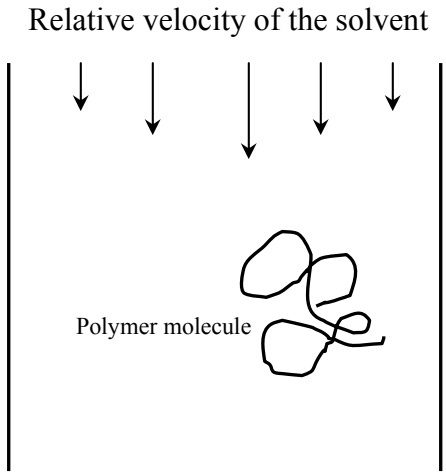

Figure 1.7.: The effect of shear rate on the polymer chain rotation (adapted from reference [39])

A Cannon-Ubbelohde Semi-Micro is a suspended level viscometer used in this project to measure the viscosity of the polymer fluids. The basic relation of capillary viscometry is Hagen–Poiseuille law, Equation 1.1,

$$\eta = \pi R^4 P / 8QL \tag{1.1}$$

where, *R* is the radius of the capillary, *P* is the hydrostatic pressure of the liquid, *Q* is the volumetric flow rate, and *L* is the length of the capillary. The bulb volume is fixed in the Ubbelohde viscometer, so, *Q*, is inversely proportional to the time, and since *P*, is proportional to the density of the fluid,

$$\eta \alpha t \rho \tag{1.2}$$

From the relation in Equation 1.2, it turns out that the flow time for a solution or solvent is proportional to the viscosity, and inversely proportional to the density. Relative viscosity is the ratio of the solution and solvent viscosities.

$$\eta_{relative} = \eta_{solution} / \eta_{solvent} \tag{1.3}$$

Since the polymeric solutions used in this project are dilute, therefore $\rho_{solution}/\rho_{solution} \sim 1$, the relative viscosity can be determined from the flow time of the solution over the flow time of the pure solvent. Since the relative viscosity is always larger than unity, specific viscosity is the relative viscosity minus one.

$$\eta_{specific} = \eta_{relative} - 1 \tag{1.4}$$

Intrinsic viscosity is the ratio of specific viscosity to the solute's concentration, extrapolated to zero concentration [39]. The inherent viscosity, $\ln \eta_{relative} / c$, and the reduced viscosity, $\eta_{specific} / c$, can be plotted against concentrations using Kraemer and Huggins equations, Equation 1.5 and Equation 1.6, respectively. Then, $\ln \eta_{relative} / c$ and $\eta_{specific} / c$ can be extrapolated to zero concentrations to find the intrinsic viscosity, $[\eta]$.

$$\eta_{specific}/c = [\eta] + k'[\eta]^2 c \tag{1.5}$$

$$(\ln \eta_{relative})/c = [\eta] - k''[\eta]^2 c \tag{1.6}$$

The values for *k'* and *k''* for many polymer-solvent systems are 0.35 and 0.15 respectively. If the *k'* and *k''* do not add up to 0.5, it can indicate molecular aggregation, ionic effects, or the existence of other problems in the system.

1.9 Scope of the Thesis

For this thesis, ELPs were expressed and purified with and without foldon and viscosity measurements were carried out over a range of concentrations and temperatures at salt concentrations less than 45 mM and greater than pH 10.2. From these viscosity measurements, the density of ELP in micelle was determined. The ELP-foldon in these conditions assembles into micelle with the hydrophobic tails phase separating into the interior of the micelle, presumably as an immiscible coacervate phase. This coacervate

contains 37% protein and 63% water in bulk phase [15]. The aim of my research is to find out the density of protein in that coacervate of the micelles by using capillary viscometry. The density of protein is assumed to be around 1.2 g/ ml, and if the coacervate has 37% protein with the rest being water, we can predict a value of density to be around 0.4 g/ ml. This density can be calculated from the intrinsic viscosity of the micelles.

CHAPTER II

MATERIALS AND METHODS

2.1 Overview

This section details the materials and methods used to prepare and characterize the proteins used in this study. Two ELP constructs were expressed and purified according to specific laboratory guidelines [37]. After the ELPs were synthesized, their concentrations were measured. Then, the viscosities of the solvent and the viscosities of different concentrations of each construct were measured over a range of temperatures.

2.2 Expression and Purification of ELPs

Elastin-like polypeptides (ELPs) used in this project are presented in Table 2.1. They were expressed and purified according to specific laboratory protocols**.** The oligomerization domain or foldon is the highlighted part of the amino acid sequences in Table 2.1. These ELPs were produced using DNA recombinant technology, to precisely control their chains lengths and amino acid sequences. Their molecular weights were calculated from the amino acid compositions.

Table 2.1: ELPs with their amino acid sequences and molecular weights.

ELP	Amino Acid Sequence	Molecular Weight (g/ mole)
$(GVGVP)_{40}$-foldon	MGH$(GVGVP)_{40}$GWPGYIP EAPRDGQAYVRKDGEWVLLSTFL	20143
$(GVGVP)_{60}$-foldon	MGH$(GVGVP)_{60}$GWPGYIP EAPRDGQAYVRKDGEWVLLSTFL	28333

2.2.1 Media Preparation

To make the media, 10 g peptone, 5 g sodium chloride, and 5 g yeast were mixed to one liter with double distilled water and the flask was autoclaved. The media was set to cool to room temperature and then 0.1 grams of ampicillin was added to media.

2.2.2 Starting Culture

A 20 ml aliquot of the prepared media was added to a culture tube and frozen stock of the desired construct was added to the tube to initiate growth. The cultures were

incubated overnight (~ 12-16 hours) at 37 ^{o}C and 300 rpm. To begin the expression, the overnight culture was added to media and cell density was monitored by BioMate 3 UV-visible spectrophotometer and when OD_{600} reached 0.8-1, expression was induced by adding 0.1 mM (240 mg) of isopropyl-β-D-thiogalactopyronoside (IPTG). The solution was shaken in an incubator for 4-5 hours at 37 ^{o}C and 300 rpm. Then, the culture was centrifuged at 10 ^{o}C and 9000 rpm and the pellet was collected.

2.2.3 Sonication

The pellets were then resuspended in phosphate buffered saline (PBS) by vortexing and were collected in a 50 ml tube. The tube was placed in ice bath and sonication was performed using 550 sonic dismembrator. The sonic dismembrator was tuned according to the manual before every sonication cycle.

2.2.4 Purification

ELPs are purified by inverse transition cycling [5]. Since the ELPs are completely soluble below their T_t, the supernatant was collected after the cold centrifugations. ELPs aggregate above their T_t, therefore the pellet was collected after hot centrifugations. Cold centrifugations were performed at 10 ^{o}C and hot centrifugations at 40 ^{o}C. After the final cycle of cold centrifugation, the liquid fraction was collected and it was filtered through a Millex GS filter with 0.22 μm pore size. In summary the steps are:

1. Cold centrifugation
2. Warm centrifugation
3. Pellet re-suspension

4. Cold centrifugation
5. Warm centrifugation
6. Pellet re-suspension
7. Cold centrifugation

2.3 Concentration Measurements

Protein concentrations were determined by using the value of the molar extinction coefficients using a procedure laid out by Gill and von Hippel [38]. The advantage of this method is that we do not need to use a large amount of our protein in order to determine its concentration. Protein concentration is measured when they are in denatured state. ELPs below their T_t are already in denatured state and therefore are ready for measurement. The concentrations of the samples were measured using a BioMate 3 UV-Visible Spectrophotometer and 1 cm x 1 cm QS quartz cuvettes at a wavelength of 280 nm. The procedure to measure the concentration of ELPs is given in Appendix A.

2.4 Verifying the Viscometer Calibration

Cannon-Ubbelohde Semi-Micro viscometer was used in this project (Figure 2.1). The constant of the viscometer (0.001909 cSt/ s) can be found in the viscometer certificate of calibration provided by the manufacturer. The constant was verified by measuring the flow time of water and comparing it to the literature values. Appendix B shows the calibration curve for the viscometer.

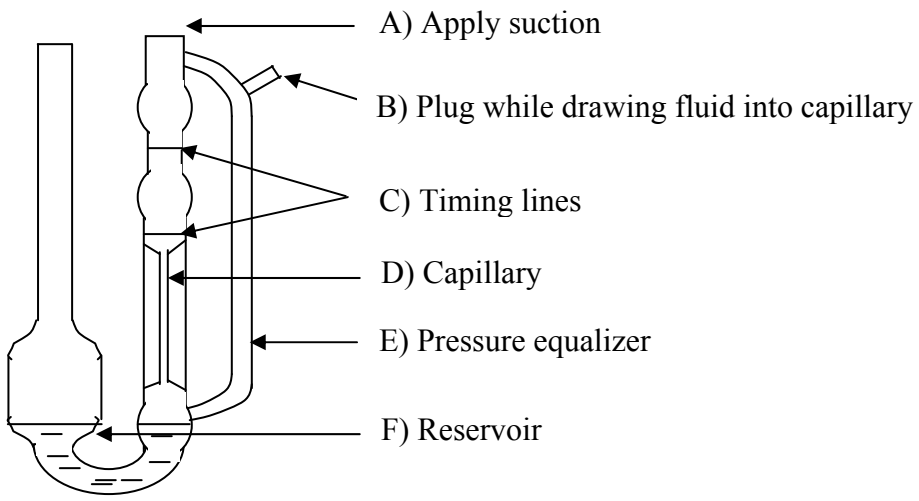

Figure 2.1.: Schematic drawing of the Cannon capillary viscometer (figure modified from reference [40]).

2.5 Flow Time Measurements

The flow time for the solvent and the ELP constructs of $(GVGVP)_{40}$-foldon, $(GVGVP)_{60}$-foldon was measured. The heating circulator in the viscometer bath was set to the temperature at which the measurement was to be taken. There was a wait of around 10 minutes after the temperature was set to allow the temperature of the bath to equilibrate (Figure 2.2). The procedure to measure the flow time of the solvent and ELP samples is given in Appendix C.

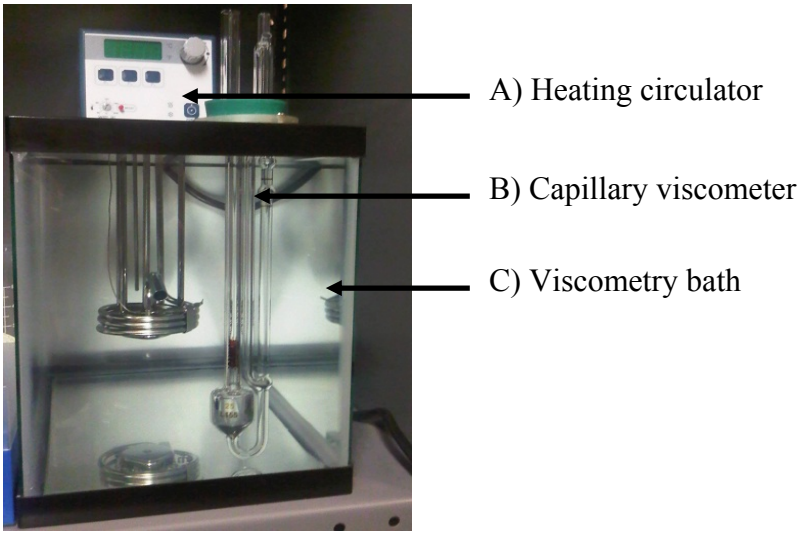

Figure 2.2.: Water bath with heating circulator and capillary viscometer (photo reproduced with permission from reference [40]).

2.6 Transition Temperature Measurements

All the transition temperature measurements were made on Shimadzu 1800 UV-vis spectrophotometer equipped with a temperature-controlled sample holder unit. A quartz cuvette was used to house the sample. A small stir bar was placed in the cuvette to perturb the sample. The spectra were obtained at 0.1 ^{o}C steps with a temperature ramp of 1 ^{o}C/ min. The measurements for the ELPs were taken for a range of temperatures starting at 25 ^{o}C and going up to 55 ^{o}C and then backwards. The spectrophotometer produces plots which show absorbance as a function of temperature. When a particular temperature caused the plot to exhibit drastically different behavior, such as much higher slope the onset of LCST was observed i.e. T_t of ELP constructs show a relatively sharp change in the 350 nm absorbance (Figure 2.3). We performed experiments on $(GVGVP)_{40}$-foldon and $(GVGVP)_{60}$-foldon. T_t values were measured as a function of ELP concentration (Figure 2.3). $(GVGVP)_{60}$-foldon does not goes into micelles above its

T_t (Figure 2.4) and hence only $(GVGVP)_{40}$-foldon was used to carry out viscosity measurements in this project.

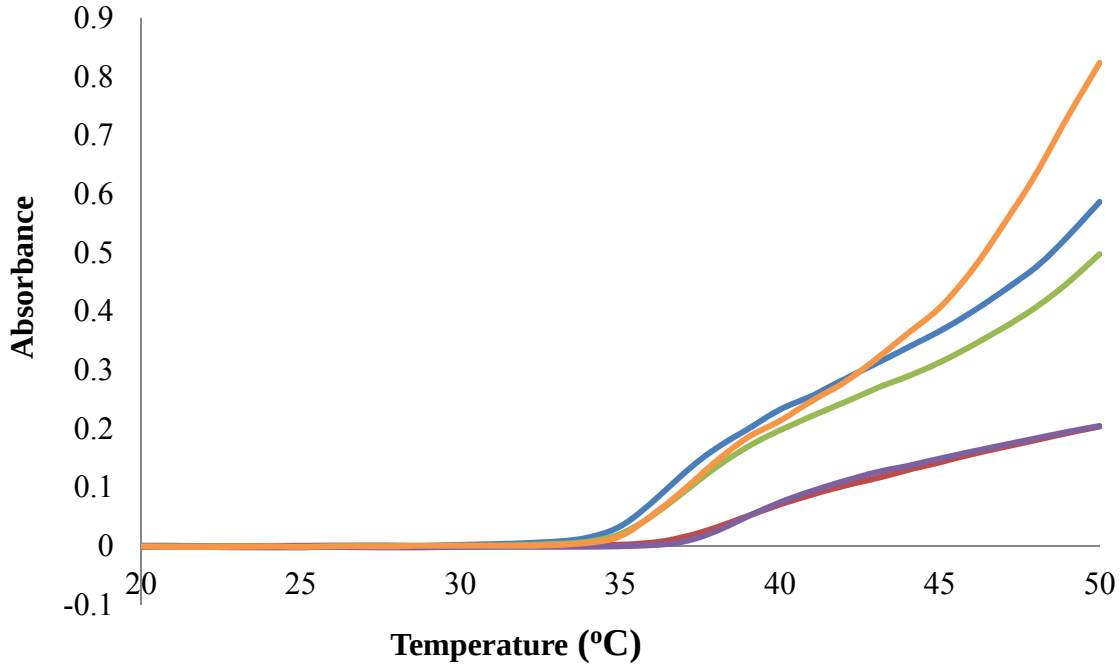

Figure 2.3.: Transition temperature of $(GVGVP)_{40}$-foldon for 853 µM (blue), 769 µM (red), 651 µM (green), 537 µM (purple), and 494 µM (orange). Figure shows the T_t dependence on concentration.

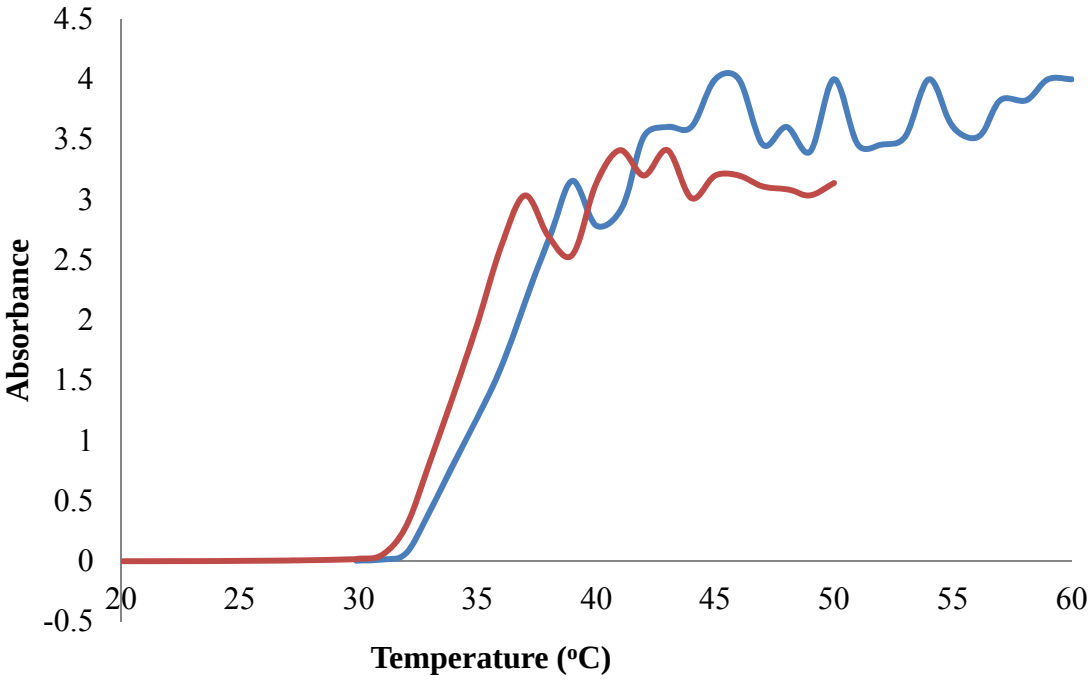

Figure 2.4.: Transition temperature of $(GVGVP)_{60}$- foldon for 583 µM (blue), and 526 µM (red). Figure shows the T_t dependence on concentration.

CHAPTER III

RESULTS AND DISCUSSION

3.1 Viscosity Calculations and Analysis

The flow times for solvent and the ELP construct solutions were obtained using the relationship based on Poiseulle's law (Equation 1.1). An empirical equation for the solvent (7.5 mM PBS) flow time as a function of temperature was fit using data from Appendix B.

$$t_{solvent}\,[s] = -5\times10^{-10}\,T^5 + 2\times10^{-7}\,T^4 - 2\times10^{-5}\,T^3 + 0.0013\,T^2 - 0.0575\,T + 1.7807 \qquad (3.1)$$

The relative viscosities of ELP samples at different concentrations were calculated based on Equation 1.5 and are shown in Figure 3.1 and Figure 3.2. These viscosity measurements were then utilized to observe the change in conformational behavior of ELPs.

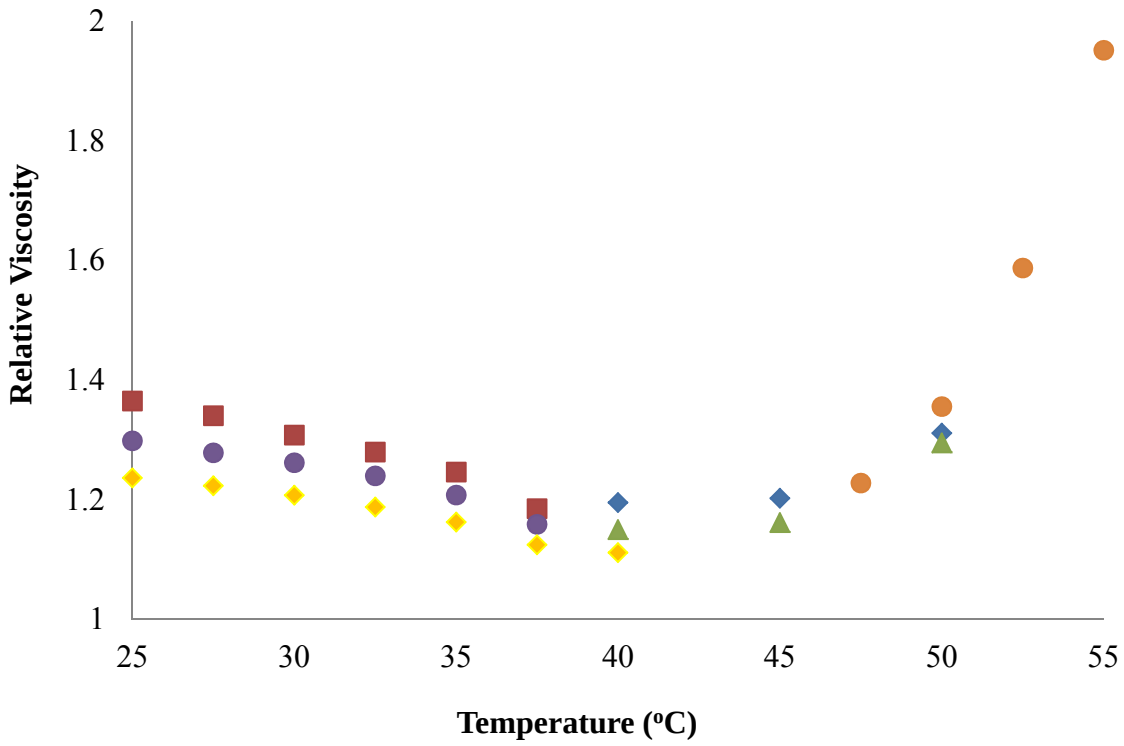

Figure 3.1.: Relative viscosity of $(GVGVP)_{40}$-foldon for 853 µM (blue diamonds), 769 µM (red squares), 650 µM (green triangles), 644 µM (purple circles), 537 µM (orange circles), and 494 µM (yellow diamonds).

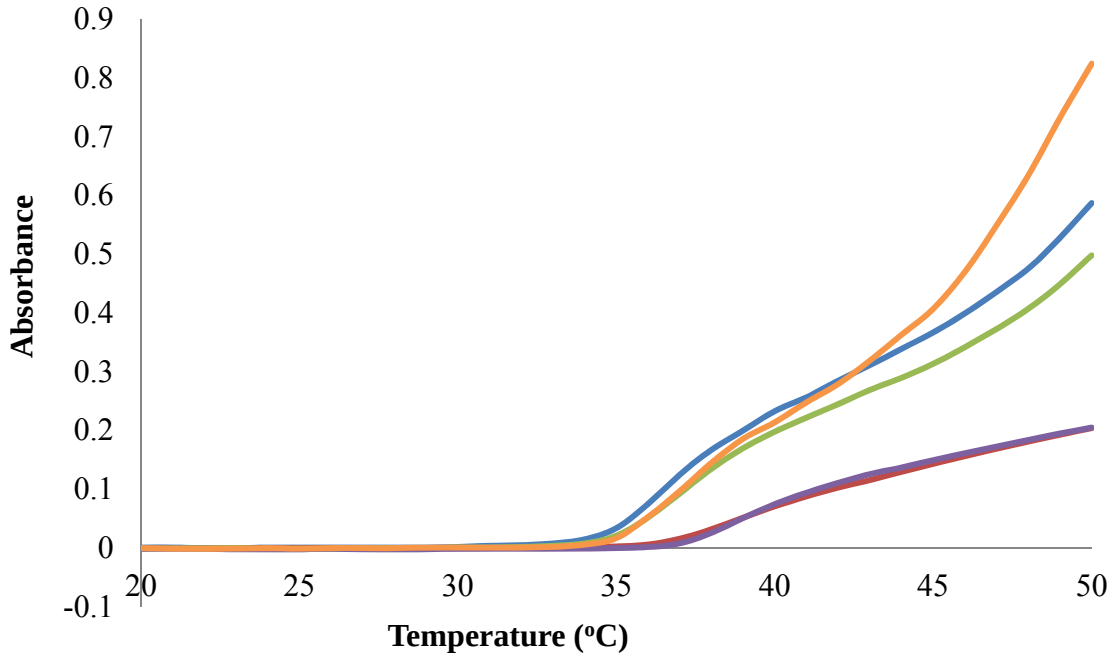

Figure 2.3.: Transition temperature of $(GVGVP)_{40}$-foldon for 853 µM (blue), 769 µM (red), 651 µM (green), 537 µM (purple), and 494 µM (orange). Figure shows the T_t dependence on concentration.

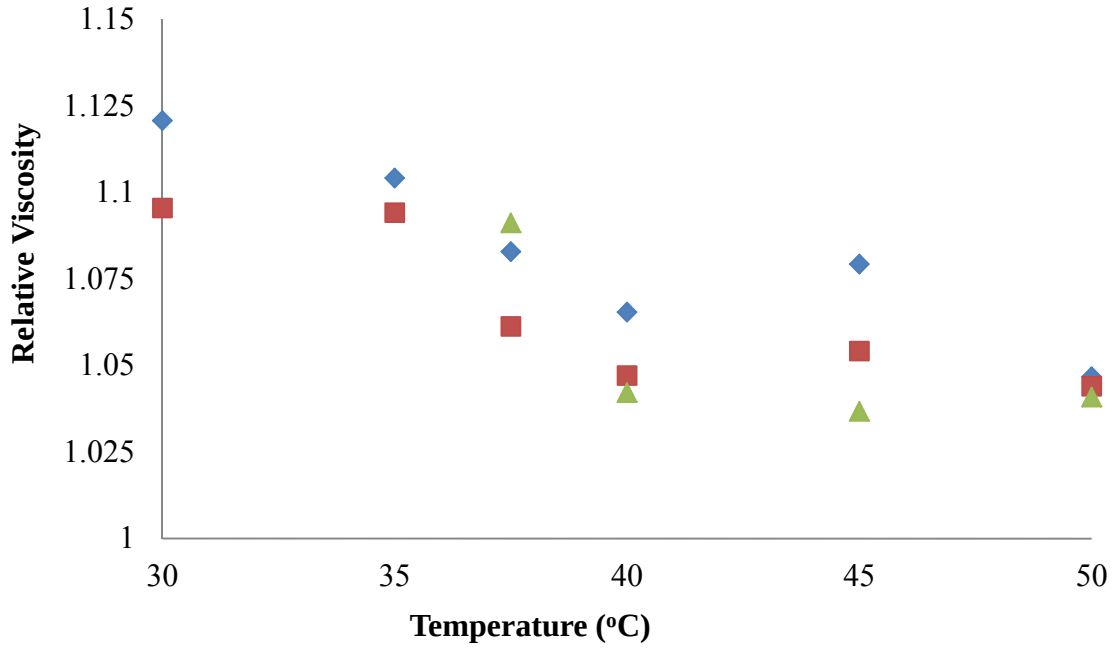

Figure 3.2.: Relative viscosity of $(GVGVP)_{40}$ -foldon for 275 µM (blue diamonds), 261 µM (red squares), and 210 µM (green triangles).

It is observed that the viscosity decreases upon an increase in the temperature or a decrease in the concentration. When the temperature increases, more of the solvent diffuses out of the polymer. The polymer becomes more compact and as a result the compact polymer produces less resistance to flow. This behavior was seen in the samples at low concentration (Figure 3.2), but the ELPs at high concentration did not follow this pattern. Figure 3.1 shows that the relative viscosity of the polymer decreases below transition temperature but above the transition temperature it starts to increase. Figure 3.2 shows the transition temperature of $(GVGVP)_{40}$-foldon over a range of concentrations. The relative and the specific viscosities are described by the Kraemer and Huggins equations [39], equation 3.2 and 3.3 respectively.

$$\eta_{specific}/c = [\eta] + k'[\eta]^2 c \tag{3.2}$$

$$(\ln \eta_{relative})/c = [\eta] - k''[\eta]^2 c \tag{3.3}$$

By using Equation 3.4, intrinsic viscosity $[\eta]$ is calculated.

$$[\eta] = \lim_{c \to 0} \eta_{specific}/c \approx \lim_{c \to 0} (\ln \eta_{relative})/c \tag{3.4}$$

The intrinsic viscosity, $[\eta]$, is the ratio of specific viscosity of the solution and the concentration of the solute extrapolated to zero. Figure 3.3 shows intrinsic viscosity by plotting Kraemer and Huggins equations. The complete sets of figures are given in Appendix D.

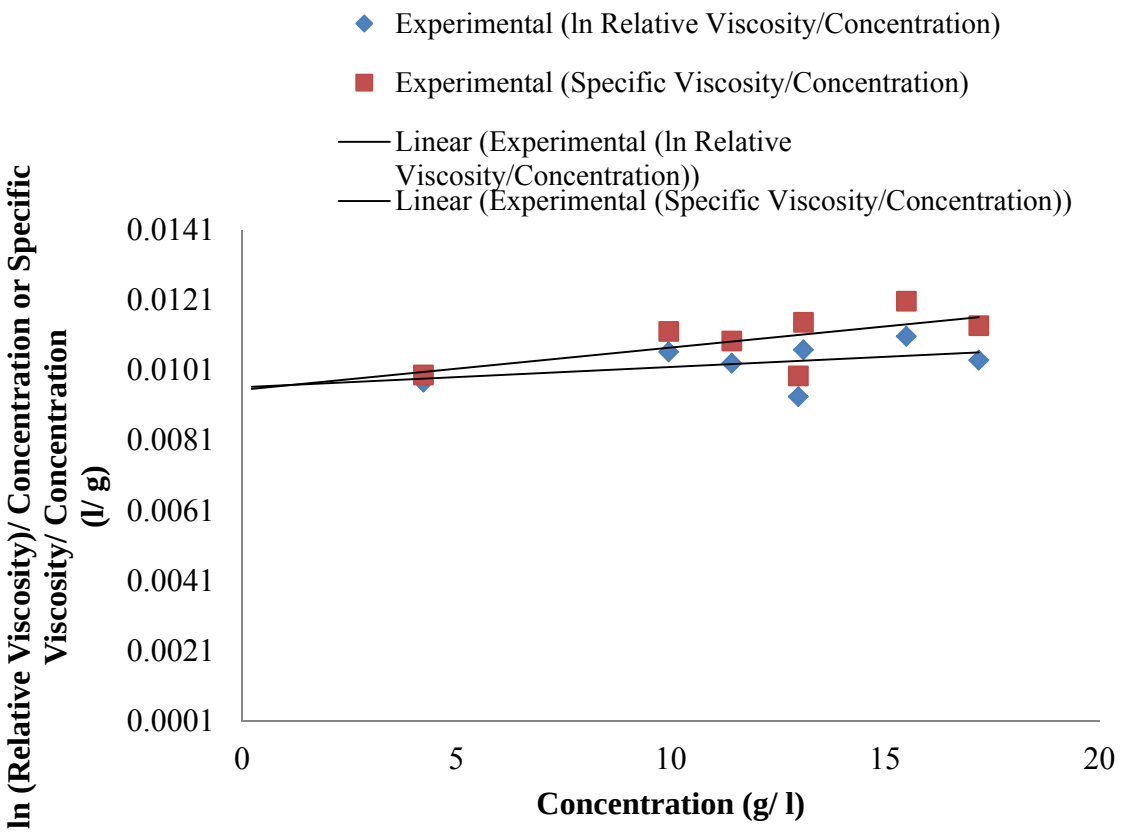

Figure 3.3.: Plot of $\eta_{specific}$/ c versus c and also (ln $\eta_{relative}$)/ c versus c for $(GVGVP)_{40}$-foldon at 40 ^{o}C extrapolated to zero concentration to find an intrinsic viscosity of 0.0107± 0.00107 l/ g.

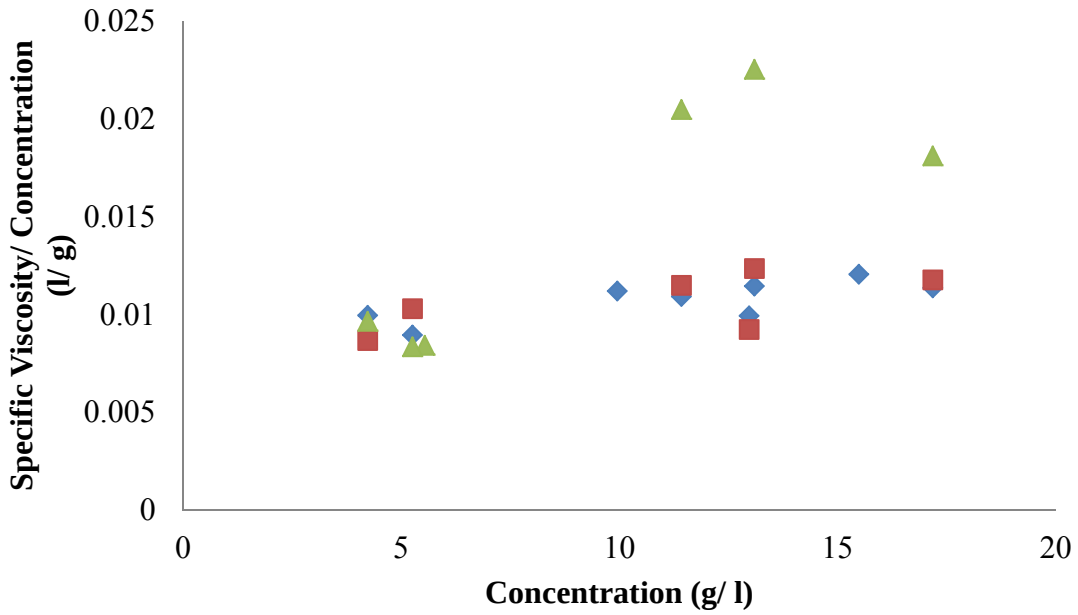

Figure 3.4.: Plot of $\eta_{specific}$/ c versus c for $(GVGVP)_{40}$-foldon at 40 ^{o}C (diamonds), 45 ^{o}C (squares) and 50 ^{o}C (triangles).

Figure 3.4. shows that the $\eta_{specific}$/ concentration for $(GVGVP)_{40}$-foldon at 40 and 45 ^{o}C overlap each other. However, this was also seen in $(GVGVP)_{40}$- foldon at 50 ^{o}C but only at lower concentrations. Specific viscosity divided by concentration increased as the concentration was increased for $(GVGVP)_{40}$-foldon at 50 ^{o}C. The summation of *k'* and *k"* for low temperature is assumed to be 0.5 and so the values for the relative viscosity are available through the experimental measurements, as a result, the Kraemer and the Huggins equations can be algebraically added to form an equation for the intrinsic viscosity based on a measurement at a single concentration.

$$[\eta] = [(\eta_{specific} - \ln \eta_{relative})/ 0.5(c)^2]^{0.5} \quad (3.5)$$

Now, the intrinsic viscosity can be determined for viscosity measurements at each concentration using Equation 3.5 (Figure 3.5). The intrinsic viscosity of $(GVGVP)_{40}$-foldon in 7.5 mM PBS exhibits a linear relationship with temperature below the T_t but above T_t this behavior is not observed.

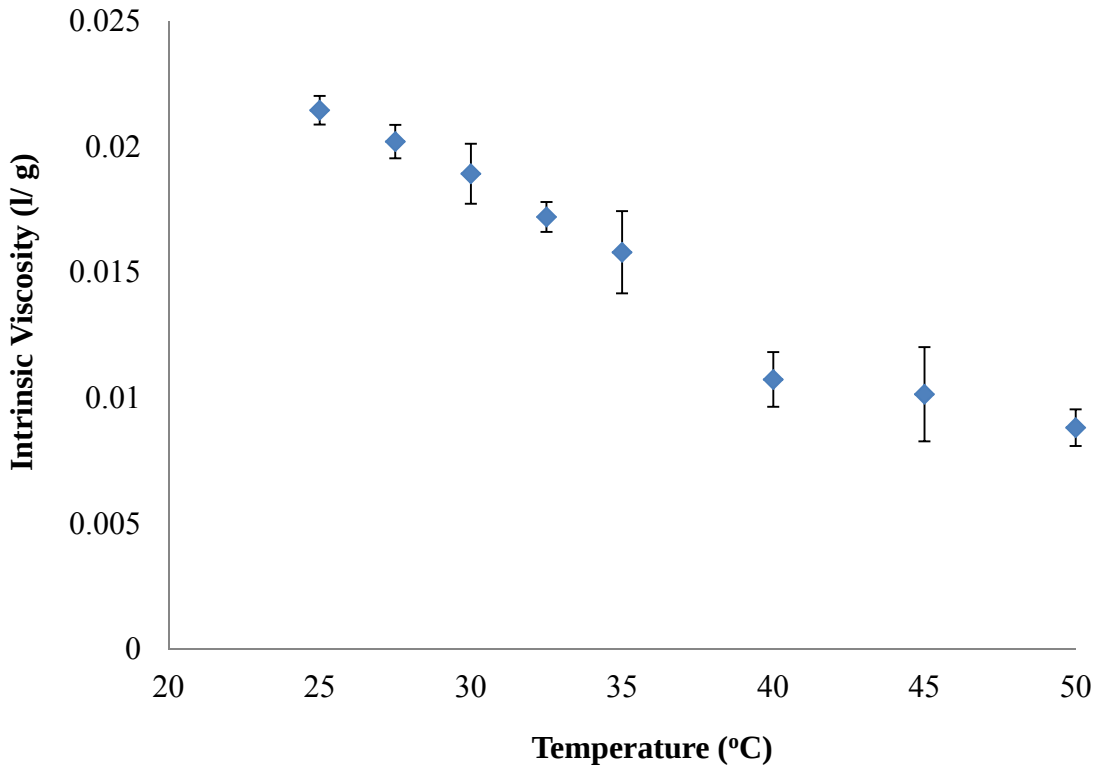

Figure 3.5.: Intrinsic viscosities of $(GVGVP)_{40}$-foldon as a function of temperature with their standard deviations.

3.2 Temperature Dependent ELP Conformational Changes

When the temperature is increased, the conformation of $(GVGVP)_{40}$ changes (Figure 3.6). ELPs are soluble at low temperatures, but above transition temperature they become insoluble. Above transition polypeptides form large particles that separate into a second phase [27]. When above the transition temperature this system acts like a surfactant and forms micelles (Figure 3.6). Micelles are small aggregates where the hydrophillic head groups surround the hydrophobic core to isolate them from the solution.

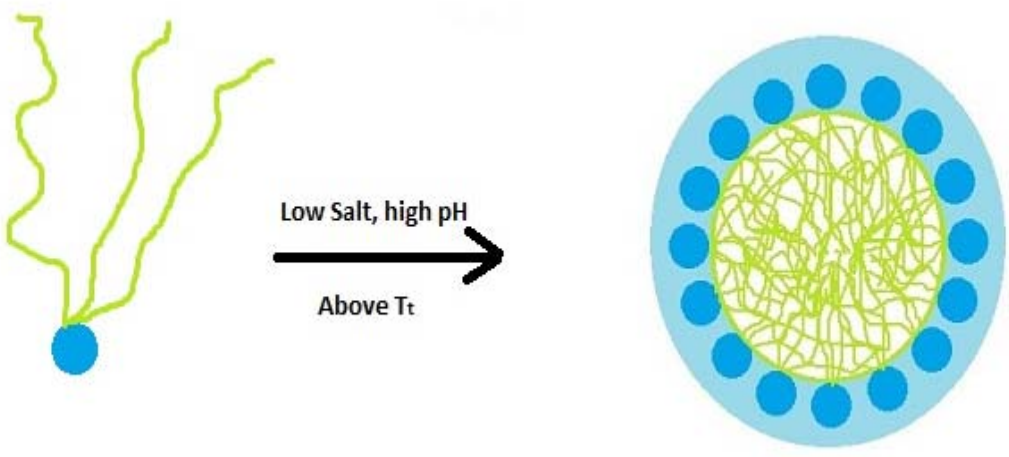

Figure 3.6.: Transition of a random coil polymer as a function of increase in temperature. The final form is a micelle above the transition temperature of the polymer.

The hydrodynamic equivalent radius of a polymer is a property that affects the viscosity of a polymer solution. Considering Einstein's expression for the viscosity in a dilute solution for uniform and non-interacting spheres in Equation 3.6, the viscosity is dependent on the volumetric fraction of the spheres in the solution. If we consider the polymers being studied acting as spheres, the hydrodynamic equivalent sphere radius (R_e) will be a measure of the sphere dimensions and Einstein's expression can be rewritten as [39]:

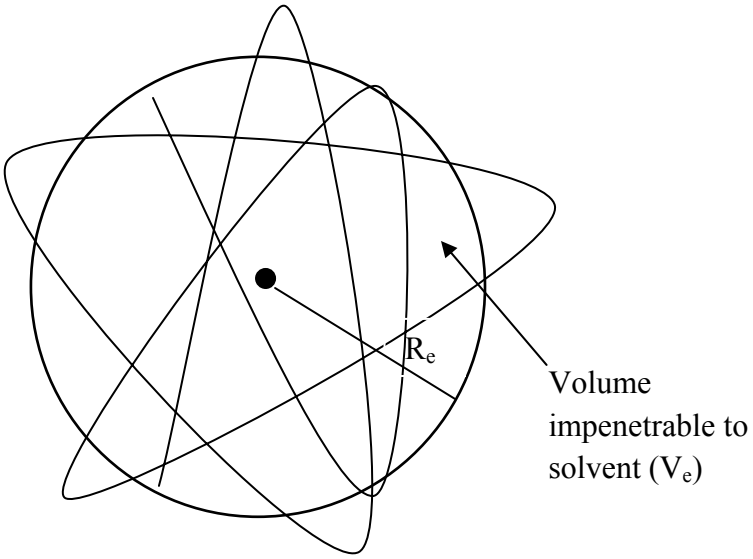

Figure 3.7.: Equivalent sphere model (adapted from reference [39])

$$\eta_{solution} = \eta_{solvent} (1+2.5v_2) \tag{3.6}$$

$$(\eta_{solution}/ \eta_{solvent} -1) = \eta_{specific} = 2.5 (n_2/ V) V_e \tag{3.7}$$

$$(n_2/ V) = c N_A/ M \tag{3.8}$$

From equation (3.7) and (3.8),

$$[\eta_{specific}/ c]_{c=0} = [\eta] = 2.5 N_A V_e/ M \tag{3.9}$$

where, n_2 is number of molecules, V is volume, V_e is equivalent sphere volume, c is mass concentration, N_A is Avogadro's number, and M is molecular weight of polymer. From Equation (3.9), we can calculate the equivalent volume, V_e. The V_e of an individual polymer can be written as $(4\pi /3) (R_e)^3$ for a spherical geometry. An increase in the equivalent radius of the polymers will yield an increase in the volumetric fraction of the spheres and that will cause an increase in intrinsic viscosity (Figure 3.8).

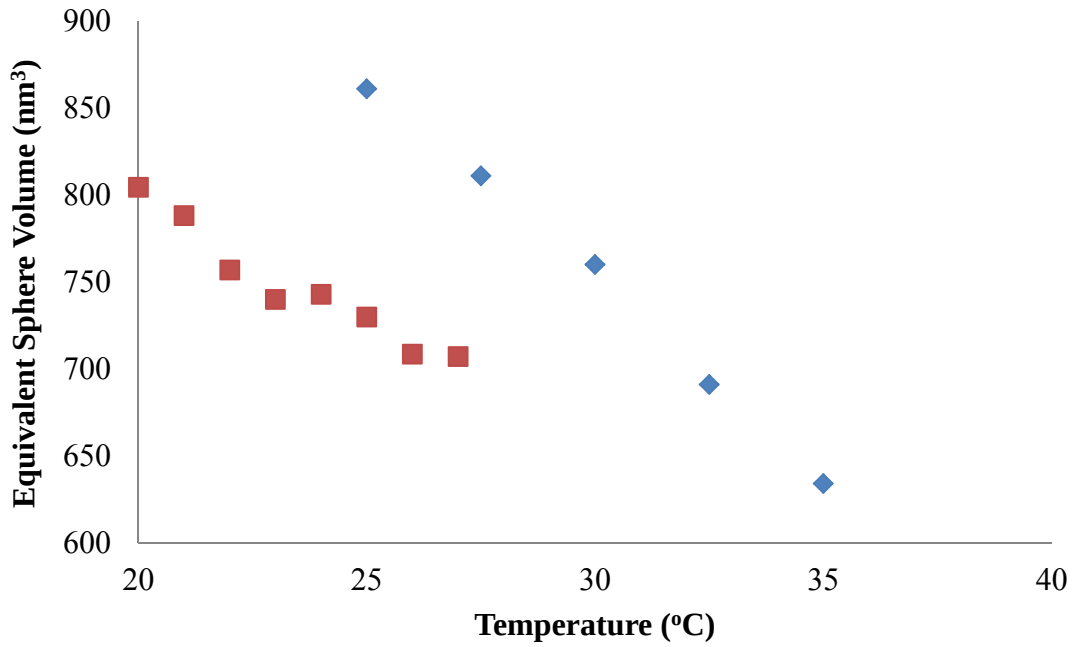

Figure 3.8.: Change of polymeric sphere equivalent volume of $(GVGVP)_{40}$-foldon as function of the temperature using equation 3.9. Squares show size in ~150 mM salt as previously published [41] compared to values measured in 7.5 mM salt and pH 10.2 (diamonds).

An increase in the temperature causes the polymer coil to become less expanded and the equivalent radius decreases. As a result the drag force on the polymers will decrease. In other words, the density of the polymer increases as a result of less expanded conformation caused by an increase in the temperature (Figure 3.8). The work done by Alanazi to characterizing ELPs using viscometry also showed that the equivalent volume of a random coli polymer decreased as the temperature increased [41]. Figure 3.8 shows that the equivalent sphere volume is larger for the random coil polymer at low salt and high pH conditions as compared with the polymer at high salt and neutral pH.

The density of protein in the coacervate is also determined using the equivalent sphere model. Coacervate is the protein rich phase in the interior of micelle where the ELP chains are collapsed together. The coacervate in the bulk has only 37% protein by

weight. The density of the coacervate is assumed to be approximately 1.2g/ ml, so the protein density should be around 0.4 g/ ml. Again, using Equation 3.6

$$\eta_{solution} = \eta_{solvent} (1+2.5v_2)$$

$$(\eta_{solution}/ \eta_{solvent} -1)/ c = (2.5v_2)/ c \quad (3.10)$$

$$[\eta_{specific} / c]_{c=0} = [\eta] = (2.5v_2)/ c \quad (3.11)$$

$$c/ v_2 = \rho_{ELP} = 2.5/ [\eta] \quad (3.12)$$

where, v_2 is volume fraction of spheres, and ρ_{ELP} is density of ELP. The density of ELP in the micelle calculated using Equation 3.12 is 0.26 ± 0.03 g/ ml which is much lower than the predicted value.

3.3 Micelle Model

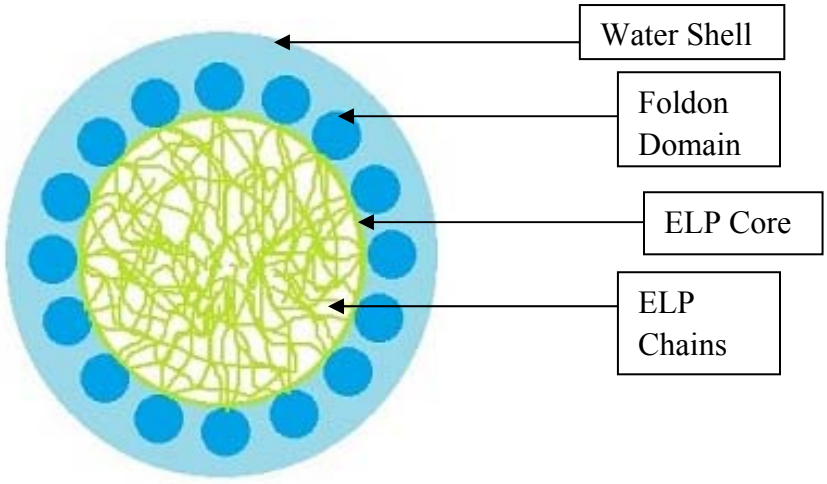

Figure 3.9.: $(GVGVP)_{40}$-foldon micelle model

$(GVGVP)_{40}$-foldon acts like a surfactant by forming micelles when it is above its transition temperature, at salt concentration less than 45 mM, and greater than pH 10 (Figure 3.9). Micelles are small aggregates where a hydrophobic portion of the surfactants are surrounded by hydrophilic head groups which isolate them from the

solution. We assume the same configuration for the $(GVGVP)_{40}$-foldon micelles where hydrophobic ELP tails phase separate in the interior of the micelle as an immiscible coacervate phase. This coacervate has 37% protein and rest is water [15]. Ghoorchian *et al.* showed that at salt concentrations below 15 mM, these micelles are spherical [27]. Data from dynamic light scattering showed that the hydrodynamic radius of these micelles is 15 nm and the weight average molecular weight of the micelles determined from static light scattering is about 4000 kD [42]. Using the intrinsic viscosity measurements, the density of ELP in the interior of micelle is 0.26 ± 0.03 g/ cm^3. The density of ELP in the micelles is calculated independently using the M_w from SLS and the hydrodynamic radius:

$$\rho = M_w / N_A V_H \tag{3.13}$$

From Equation 3.13, the density is 0.47 g/ cm^3 assuming that the weight measured by SLS is all protein. This difference in density indicates that the M_w measured by SLS includes the water that is bound in the micelle, suggesting that that the core contains significant amount of water.

From the density determined from intrinsic viscosity and the hydrodynamic radius measured by DLS we can caluclate the molecular weight of protein in a micelle:

$$M_{protein} = \rho_{micelle} N_A V_H \tag{3.14}$$

where, $M_{protein}$ is the molecular weight of the protein and $\rho_{micelle}$ is the density of protein in the micelle, 0.26 ± 0.03 g/ cm^3. The molecular weight of protein calculated using Equation 3.14 is 2220 ± 210 kD. So, we can now also calculate the molecular weight of water:

$$M_{SLS} = M_{protein} + M_{H2O} \tag{3.15}$$

$$M_{H2O} = M_{SLS} - M_{protein} \quad (3.16)$$

The resulting molecular weight of water from Equation 3.16 is 1780 ± 190 kD. Assuming all of the tightly bound water is in the core that the core has 40 ± 4 % protein. This is in close agreement with the bulk coacervate, which reportedly has 37% [15]. In this model, we assume that the micelles are non- interacting spheres in the solution. Figure 3.10. shows a micelle in solution where hydrophilic headgroups surround the ELP core. Inside the ELP core, we found that the coacervate has 40 ± 4 % protein and rest water. From the density of protein in the micelle, we can also calculate the mass of protein in micelle and the number of $(GVGVP)_{40}$-foldon (n_2) in the micelle.

$$Mass_{protein} = \rho_{micelle} / V_M \quad (3.17)$$

$$n_2 = (Mass_{protein}) N_A / M \quad (3.18)$$

The number of $(GVGVP)_{40}$-foldon molecules per micelle is 110 ± 11, which is three times. The number of trimers in the micelle, is 37 ± 4. Using the micelle model, we can also calculate the radius of ELP core.

$$R_{core} = (3V_{core} / 4\pi)^{1/3} \quad (3.19)$$

where, V_{core} is mass of core/ density of coacervate. The radius of ELP core calculated using Equation 3.19 is 11.9 ± 2 nm. We know the diameter of the headgroup i.e. 2 nm [27]. So, we can calculate the thickness of water shell around the micelle.

$$Thickness_{water\ shell} = R_H - (R_{ELP\ core} + D_{headgroup}) \quad (3.20)$$

where, R_H is the hydrodynamic radius determined using DLS, $R_{ELP\ core}$ is radius of ELP core and $D_{headgroup}$ is diameter of the headgroup. The thickness of water shell around the micelle calculated using Equation 3.20 is ≤ 1.1 nm.

CHAPTER IV

CONCLUSIONS

An empirical formula for the efflux time of 7.5 mM PBS as a function of temperature and the intrinsic viscosity for $(GVGVP)_{40}$-foldon in 7.5 mM PBS as function of temperature were made from viscosity measurements. Viscosity measurements for $(GVGVP)_{60}$- foldon in 7.5 mM PBS were not carried out because it aggregates above its T_t instead of forming micelles. For $(GVGVP)_{40}$-foldon, the micelles at high concentrations and above 47.5 ^{o}C were not non- interacting spheres, but showed a dramatic increase in viscosity. Using the equivalent sphere model for non-interacting spheres, the density of protein in the micelle was calculated from intrinsic viscosity for lower concentrations and lower temperatures. A micelle model for $(GVGVP)_{40}$-foldon was developed. Using this model, we calculated the density of protein in the coacervate and our results were in close proximity with the literature. From the density of protein, we were able to tell about the number of trimers which make up the ELP core in the micelle. Using our micelle model, we were also able to estimate the thickness of water

shell surrounding the micelle. There were two limitations in this project. First, the flow time of polymer solution at low concentrations produced specific viscosity close to zero, therefore increasing the error value. Second, the pH of the sample decreased during the course of experiment and there was no provision in the viscometer for adjusting the pH of the sample. Future work should be carried out by closely monitoring the pH during the experiment.

BIBLIOGRAPHY

[1] Meyer, Dan E. and Chilkoti, Ashutosh. "Genetically Encoded Synthesis of Protein-Based Polymers with Precisely Specified Molecular Weight and Sequence by Recursive Directional Ligation: Examples from the Elastin-like Polypeptide System." *Biomacromolecules* 3.2, **(2002)**.

[2] Urry, Dan W. "Physical Chemistry of Biological Free Energy Transduction As Demonstrated by Elastic Protein-Based Polymers." *Journal of Physical Chemistry B* 101.51, **(1997)**.

[3] Circulis, Judith T. and Keeley, Fred W. "Viscoelastic properties and gelation of an elastin-like polypeptide." *The Society of Rheology*, **(2009)**.

[4] http://www.worldscibooks.com/chemistry/P297.html.

[5] McPherson, David T., Xu, Jie, Urry, Dan W. "Product Purification by Reversible Phase Transition following Escherichia coli Expression of Genes Encoding upto 251 Repeats of the Elastomeric Pentapeptide GVGVP." *Protein Expression and Purification* 7, **(1996)**.

[6] Liu, W., Dreher, M. R., Furgeson, D. Y., Peixoto, K. V., Yuan, H., Zalutsky, M. R., and Chilkoti, Ashutosh. "Tumor accumulation, degradation and pharmacokinetics of elastin-like polypeptides in nude mice." *Journal of Controlled Release* 116.2, **(2006)**.

[7] Laromaine, A., Koh, L., Murugesan, M., Ulijn, R. V., and Stevens M. "Protease-Triggered Dispersion of Nanoparticle Assemblies." *Journal of the American Chemical Society* 129.14, **(2007)**.

[8] Chow, Dominic, Nunalee, M., Lim, D. W., Simnick, A. J., and Chilkoti, Ashutosh. "Peptide-based biopolymers in biomedicine and biotechnology." *Materials Science & Engineering R* 62.4, **(2008)**.

[9] Paiva, L. R. and Martins, M. L. "A multiscale model to evaluate the efficacy of anticancer therapies based on chimeric polypeptide nanoparticles." *Applied Physics Letters* 98.5, **(2011)**.

[10] Adams, Samuel B., Shamji, Mohammed., Nettles, Hwang F., Priscilla, Dana L., and Setton, Lori. "Sustained release of antibiotics from injectable and thermally responsive polypeptide depots." *Journal of Biomedical Materials Research Part B: Applied Biomaterials* 90B.1, **(2009)**.

[11] Sorg, Brian., Peltz, Cathryn D., Klitzman, Bruce., and Dewhirst, Mark. "Method for improved accuracy in endogenous urea recovery marker calibrations for microdialysis in tumors." *Journal of Pharmacological and Toxicological Methods* 52.3, **(2005)**.

[12] Temming, Kai., Schiffelers, Raymond., Molema, Grietje, and Robbert J. Kok. "RGD-based strategies for selective delivery of therapeutics and imaging agents to the tumor vasculature." *Drug Resistance Updates* 8.6, **(2005)**.

[13] Betre, Helawe, Liu, Wenge, Zalutsky, Michael R., Chilkoti, Ashutosh, Kraus, Virginia, and Lori Setton. "A thermally responsive biopolymer for intra-articular drug delivery." *Journal of Controlled Release* 115.2, **(2006)**.

[14] Kemppainen, Barbara., Urry, Dan W., Luan, Chi-Xiang., Xu, Jie., Swaim, Steven., and Goel, Saryu. "In vitro skin penetration of dazmegrel delivered with a bioelastic matrix." *International Journal of Pharmaceutics* 271.1-2, **(2004)**.

[15] Urry, Dan W. “Entropic Elastic Process in Protein Mechanisms. I. Elastic Structure Due to an Inverse Temperature Transition and Elasticity Due to Internal Chain Dynamics.” *Journal of Protein Chemistry*, Vol. 7, No. 1, **(1988).**

[16] Girotti, A., and Reguera, J. “Influence of the Molecular Weight on the Inverse Temperature Transition of a Model Genetically Engineered Elastin-like pH Responsive Polymer, *Macromolecules*, **(2004)**.

[17] Reguera, J., Urry, Dan W., Parker, T.M., McPherson, D.T., Rodriguez Cabello, J.C. “Effect of NaCl on the Exothermic and Endothermic Components of the Inverse Temperature Transition of a Model Elastin-like Polymer.” *Biomacromolecules*, **(2007)**.

[18] Reguera, J., Urry, Dan W., Parker, T.M., McPherson, D.T., Rodriguez Cabello, J.C. “Endothermic and Exothermic Components of an Inverse Temperature Transition for hydrophobic association by TMDSC.” *Journal of Chemical Physical Letters*, **(2004)**.

[19] Nuhn, H., and Klok, H.A. “Secondary Structure Formation and LCST Behavior of Short Elastin-like Peptides.” *Biomacromolecules*, **(2008)**.

[20] Urry, Dan W., Long, M., and Sugano, H. “Cyclic Analog of Elastin polyhexapeptide exhibits an Inverse Temperature Transition leading to Crystallization.” *Journal of Biological Chemistry*, **(1978)**.

[21] Pechar, M., Brus, J., Kostka, L., and Konak, C. “Thermoresponsive self-assembly of short elastin-like polypentapeptides and their poly(ethylene glycol) derivatives.” *Macromolecular Bioscience*, **(2007)**.

[22] Van Hest, J.C., Ayres, L., Koch, K., and Adams, P. "Stimulus Responsive Behavior of Elastin- based Side Chain Polymers." *Macromolecules*, **(2005)**.

[23] Luan, C.H., Parker, T.M., Urry, Dan W., and Prasad, K.U. "Differential scanning calorimetry studies of NaCl effects on the Inverse Temperature Transition of some Elastin-based polytetra, polypenta and polynanopeptides." *Biopolymers*, **(1991)**.

[24] Yamaoka, T., Tamuar, T., Seto, Y., Tada, T., Kunugi, S., and Tirrell, D. "Mechanism for the Phase Transition of a Genetically Engineered Elastin Model Peptide $(VPGIG)_{40}$ in aqueous solution." *Biomacromolecules*, **(2003)**.

[25] Zhang, Y., Trabbic-Carlson, K., Albertorio, F., Chilkoti, A., and Cremer, P.S. "Aqueous Two-Phase System Formation Kinetics for Elastin-like Polypeptides of Varying Chain Length." *Biomacromolecules*, **(2006)**.

[26] Von Hippel, P.H., and Wong, K.Y. "On the conformational stability of globular proteins. The effects of various electrolytes and nonelectrolytes on the thermal ribonuclease transition." *Journal of Biological Chemistry*, **(1965)**.

[27] Ghoorchian, Ali., Cole, James T., and Holland, Nolan B. "Thermoreversible Micelle Formation Using a Three-Armed Star Elastin-like Polypeptide." *Macromolecules* 43.9, **(2010)**.

[28] Urry, Dan W., Trapane, T.L., and Prasad, K.U. "Phase- Structure Transitions of the Elastin Polypentapeptide- Water system within the Framework of Composition- Temperature Studies." *Biopolymers*, **(1985)**.

[29] Meyer, D.E., and Chilkoti, A. “Quantification of the Effects of Chain length and Concentration on the Thermal Behavior of Elastin-like Polypeptides.” *Biomacromolecules*, **(2004)**.

[30] Urry, Dan W. “Molecular Machines: how motion and other functions of living organisms can result from reversible chemical changes.” *Angew Chem Int Ed Engl*, **(1993)**.

[31] MacKay, J. Andrew, Callahan, Daniel J., FitzGerald, Kelly N., and Chilkoti, Ashutosh. “Quantitative Model of the Phase Behavior of Recombinant pH-Responsive Elastin-Like Polypeptides.” *Biomacromolecules* 11.11, **(2010)**.

[32] MacEwan, S., and Hassouneh, W. “Elastin-like Polypeptides: Biomedical Applications.” **(2010)**.

[33] Dreher, Matthew R., Simnick, Andrew J., Fischer, Karl, Smith, Richard J., Patel, Anand, Schmidt, Manfred, and Chilkoti, Ashutosh,“Temperature Triggered Self-Assembly of Polypeptides into Multivalent Spherical Micelles.” *J Am Chem Soc.* **(2008)**.

[34] Pellarin, Riccardo and Caflisch., Amedeo. “Interpreting the Aggregation Kinetics of Amyloid Peptides.” *Journal of Molecular Biology* 360.4, **(2006)**.

[35] Pappu, Rohit V., Wang, Xiaoling, Vitalis, Andreas, and Crick, Scott L. “A polymer physics perspective on driving forces and mechanisms for protein aggregation.” *Archives of Biochemistry and Biophysics* 469.1, **(2008)**.

[36] Bochicchio, Brigida., Pepe, Antonietta. and Tamburro, Antonio M. “Investigating by CD the molecular mechanism of elasticity of elastomeric proteins.” *Chirality* 20.9, **(2008)**.

[37] Tamburro, Antonio Mario., Lorusso, Marina., Ibris, Neluta., Pepe, Antonietta., and Bochicchio, Brigida. "Investigating by Circular Dichroism some Amyloidogenic Elastin-derived Polypeptides ." *Chirality* 22.1E, **(2010)**.

[38] Gill, S.C., and von Hippel, P.H. "Calculation of Protein Extinction Coefficients from Amino Acid Sequence Data." **(1989)**.

[39] Sperling, L. H. "Introduction to Physical Polymer Science." Hoboken, NJ: Wiley, **(2006)**.

[40] Russo, P. "IntrinsicVisc.doc" **(2008)**.

[41] Alanazi, Hamdan. "Characterization of Elastin-Like Polypeptides using Viscometry." **(2011)**.

[42] Ghoorchian, Ali. "Modification of Behavior of Elastin-Like Polypeptides by changing Molecular Architecture." **(2012)**.

APPENDIX

APPENDIX A

(Procedure for Measuring Protein Concentration)

The procedure for taking measurements is as follows:

- Measure blank sample of 1 ml 7.5 mM salt PBS.
- Make 10% protein sample in 7.5 mM salt PBS by adding 100 µl protein to 900 µl 7.5 mM salt PBS.
- Make 5% - 1.25% protein sample by removing 500 µl of sample from the cuvette and adding 500 µl of 7.5 mM salt PBS.
- Record measurements and determine if the measurements follow a linear decrease, i.e. 5% concentration measurement should be half of the 10% concentration measurement.

APPENDIX B

(Viscometer Constant Calibration)

The constant for the viscometer was verified through comparing the literature and the experimental measurements and it was calculated to be 0.001909 cSt/ s.

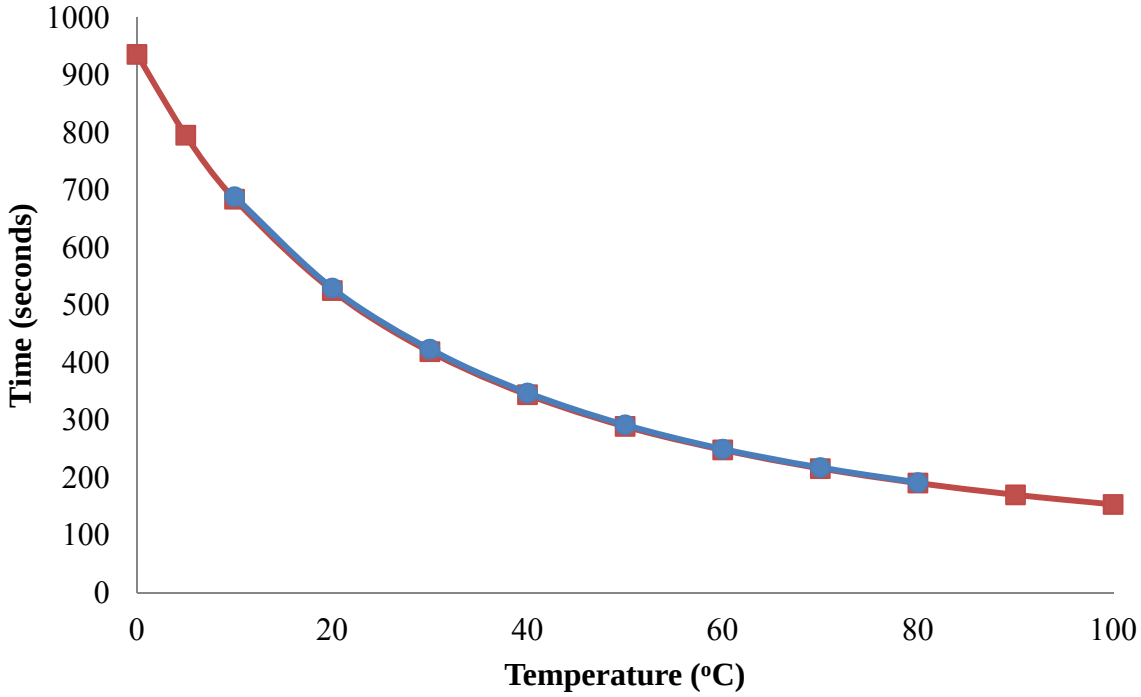

Figure B.1.: Calibration curve for capillary viscometer. The red curve denotes the time taken for water to travel through a capillary in literature. The blue curve denotes the experimental time.

APPENDIX C

(Procedure for Measuring Flow Time)

- Place the Cannon-Ubbelohde Semi-Micro viscometer (Figure 2.1) in the viscometer bath (Figure 2.2). The viscometer should be washed with distilled water and completely dried.
- Video recorder is turned on and aligned with the upper timing line of the viscometer.
- A known amount of water or solvent or ELP is loaded in the viscometer.
- Set the viscometer bath to a desired temperature.
- Allow 10 minutes for equilibration.
- Once the targeted temperature is reached suction is applied at point A in Figure 2.1 while point B is plugged with the thumb.
- As the solution passes the upper timing line, video recording is started. Also, the stopwatch is turned on.
- After the solution passes the lower timing line, stopwatch is stopped and flow time is recorded.
- Repeat the steps above to take a second measurement to confirm the accuracy of the data.
- If the flow times for the two measurements are not in agreement, repeat the steps for a third measurement. Fourth measurement might also be conducted if necessary.

- Change the temperature of the heating circulator and wait for the temperature in the viscometer bath to reach equilibrium.
- Then, repeat the same procedure.
- Obtain measurements for the desired range of temperature.
- After all measurements are taken, the video recorder and the heating circulator are turned off. Then, the solution is emptied in a falcon tube and the viscometer is cleaned with distilled water and dried with vacuumed air.
- Finally, the video recording is analyzed to obtain the recorded timing for each measurement.

APPENDIX D

(Intrinsic Viscosity Graphs)

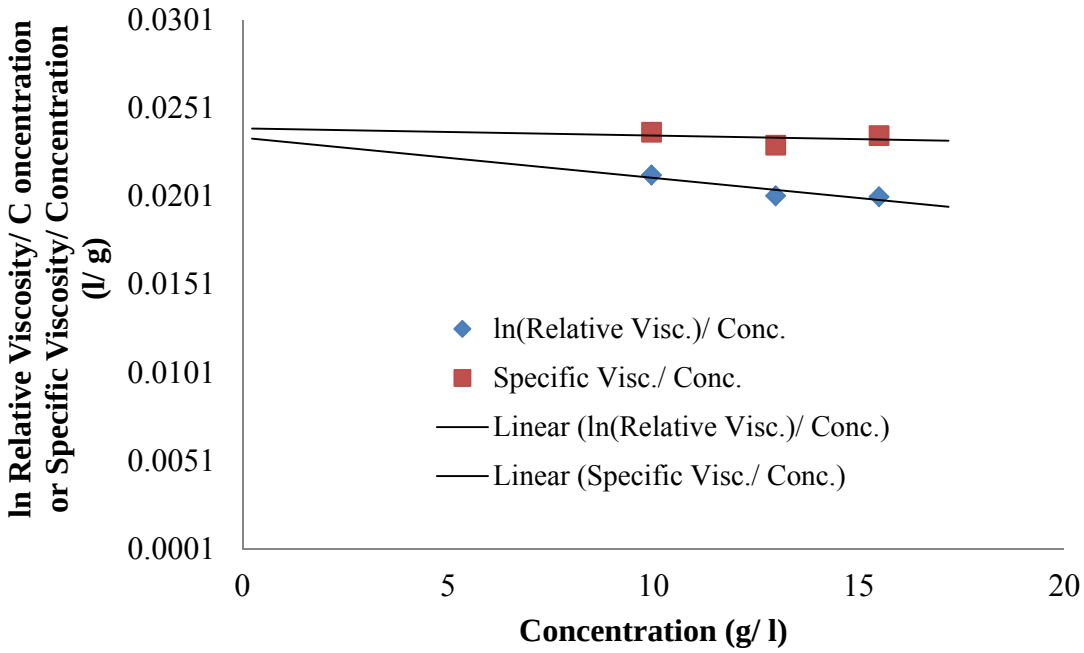

Figure D.1.: Plot of $\eta_{specific}$/ c versus c and also (ln $\eta_{relative}$)/ c versus c for $(GVGVP)_{40}$-foldon at 25 ^{o}C extrapolated to zero concentration to find an intrinsic viscosity of 0.0215 l/ g .

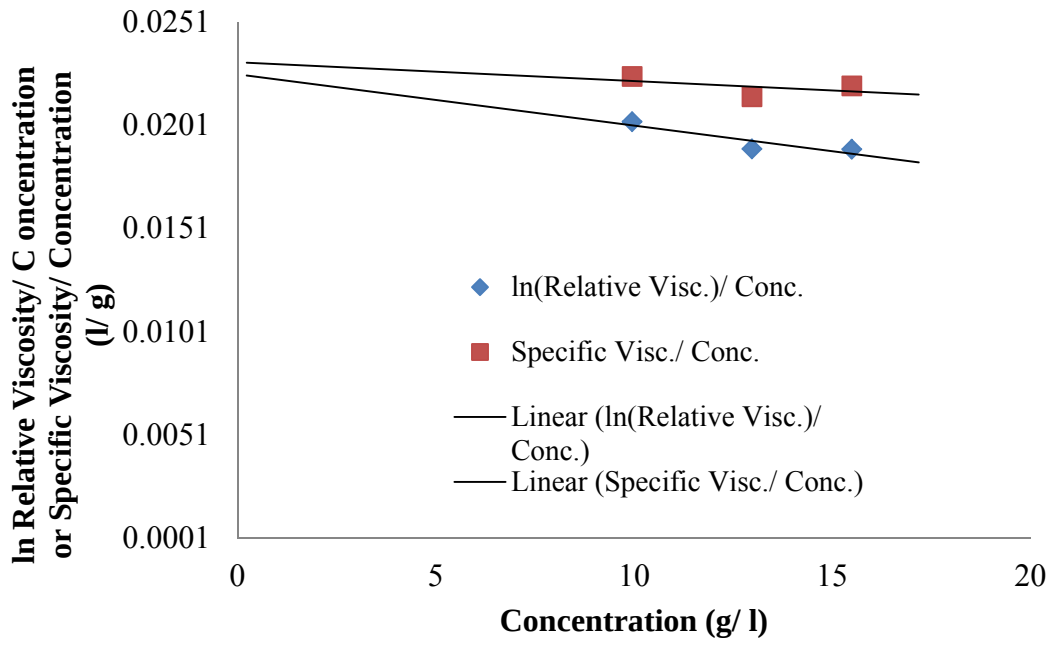

Figure D.2.: Plot of $\eta_{specific}$/ c versus c and also (ln $\eta_{relative}$)/ c versus c for $(GVGVP)_{40}$-foldon at 27.5 ^{o}C extrapolated to zero concentration to find an intrinsic viscosity of 0.0202 l/ g .

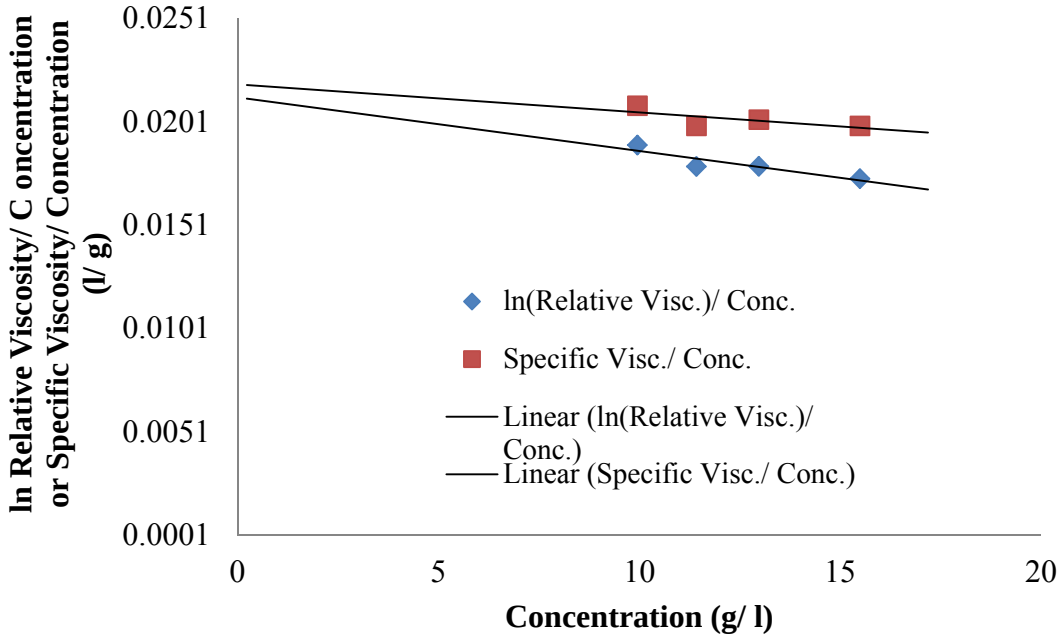

Figure D.3.: Plot of $\eta_{specific}$/ c versus c and also (ln $\eta_{relative}$)/ c versus c for $(GVGVP)_{40}$-foldon at 30 ^{o}C extrapolated to zero concentration to find an intrinsic viscosity of 0.019 l/ g .

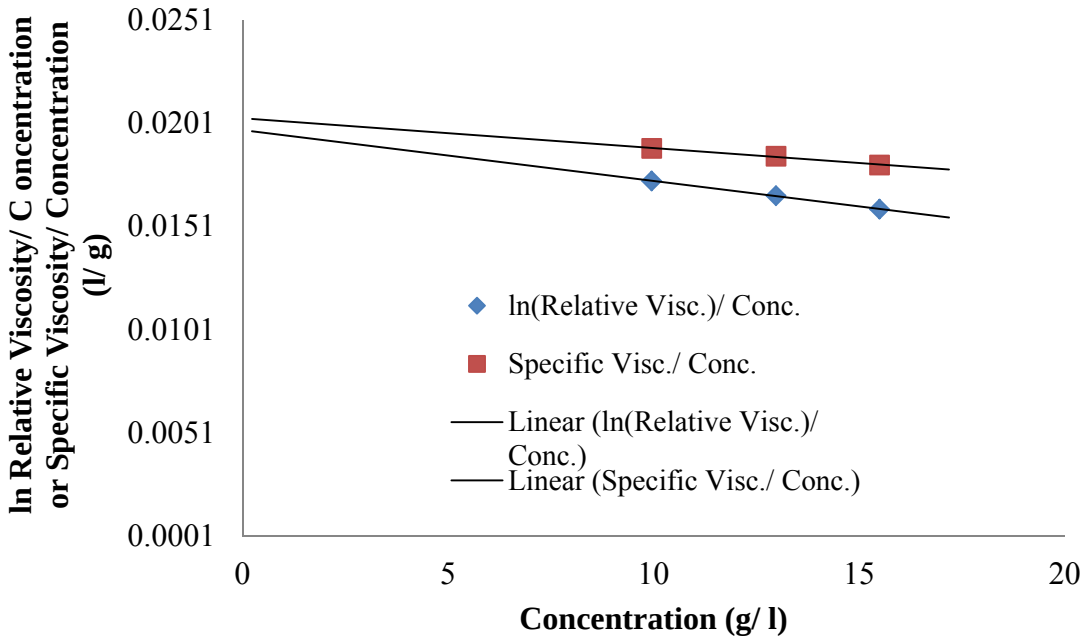

Figure D.4.: Plot of $\eta_{specific}$/ c versus c and also (ln $\eta_{relative}$)/ c versus c for $(GVGVP)_{40}$-foldon at 32.5 ^{o}C extrapolated to zero concentration to find an intrinsic viscosity of 0.0172 l/ g.

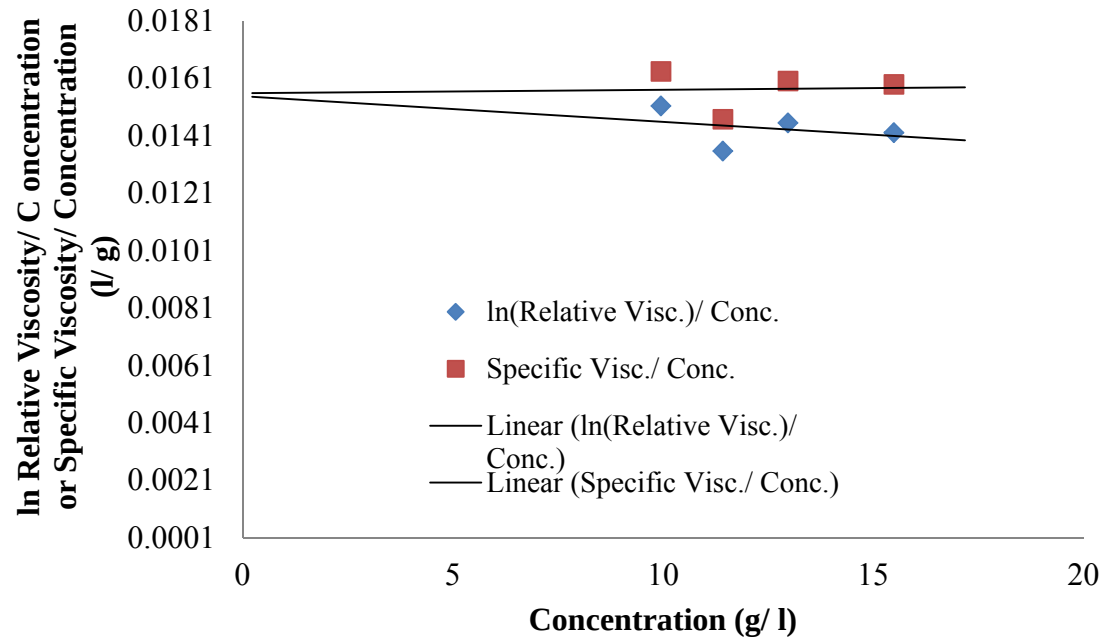

Figure D.5.: Plot of $\eta_{specific}$/ c versus c and also (ln $\eta_{relative}$)/ c versus c for $(GVGVP)_{40}$-foldon at 35 ^{o}C extrapolated to zero concentration to find an intrinsic viscosity of 0.0158 l/ g.

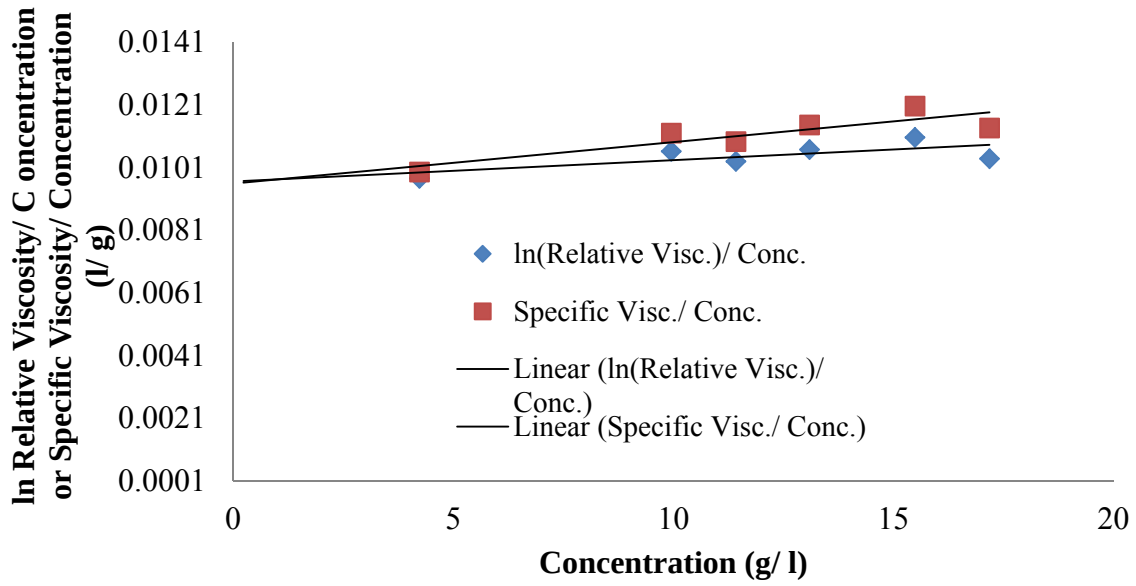

Figure D.6.: Plot of $\eta_{specific}$/ c versus c and also (ln $\eta_{relative}$)/ c versus c for $(GVGVP)_{40}$-foldon at 40 ^{o}C extrapolated to zero concentration to find an intrinsic viscosity of 0.0107 l/ g .

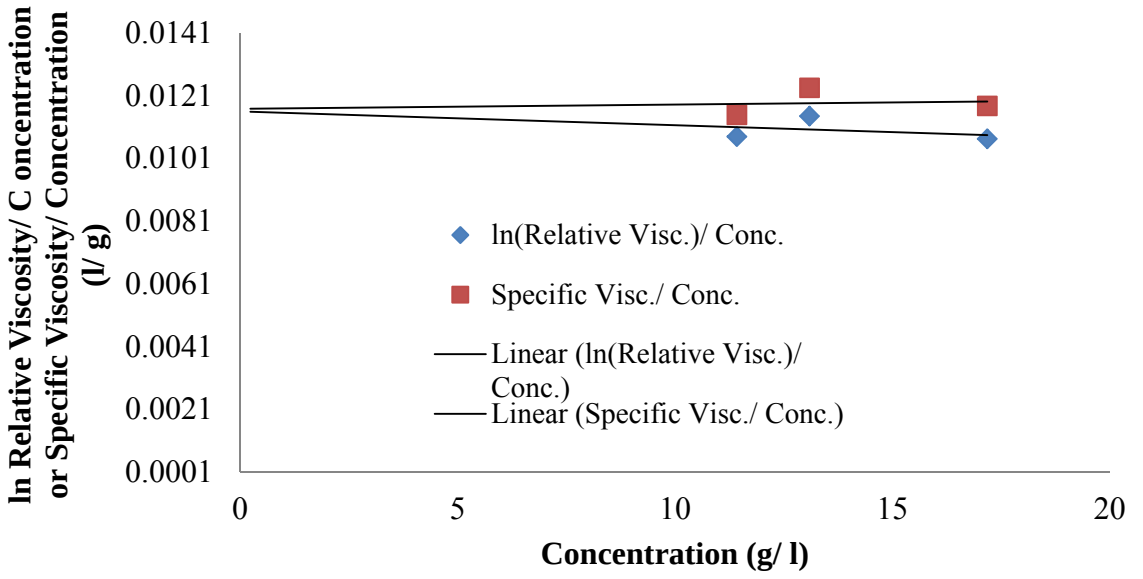

Figure D.7.: Plot of $\eta_{specific}$/ c versus c and also (ln $\eta_{relative}$)/ c versus c for $(GVGVP)_{40}$-foldon at 45 ^{o}C extrapolated to zero concentration to find an intrinsic viscosity of 0.01015 l/ g.

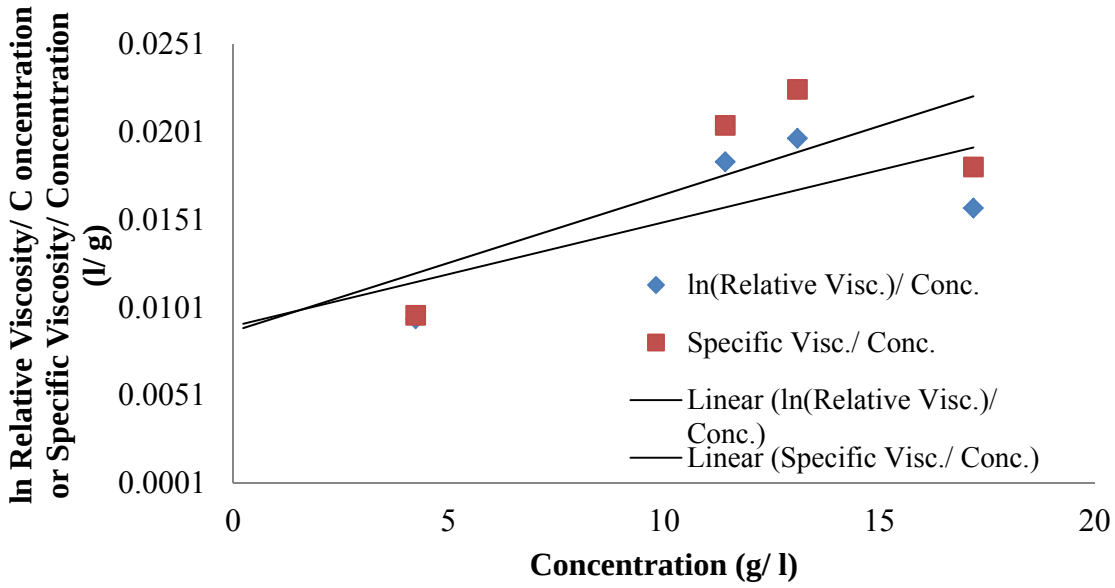

Figure D.8.: Plot of $\eta_{specific}/c$ versus c and also $(\ln \eta_{relative})/ c$ versus c for $(GVGVP)_{40}$-foldon at 50 °C extrapolated to zero concentration to find an intrinsic viscosity of 0.00882 l/ g.